



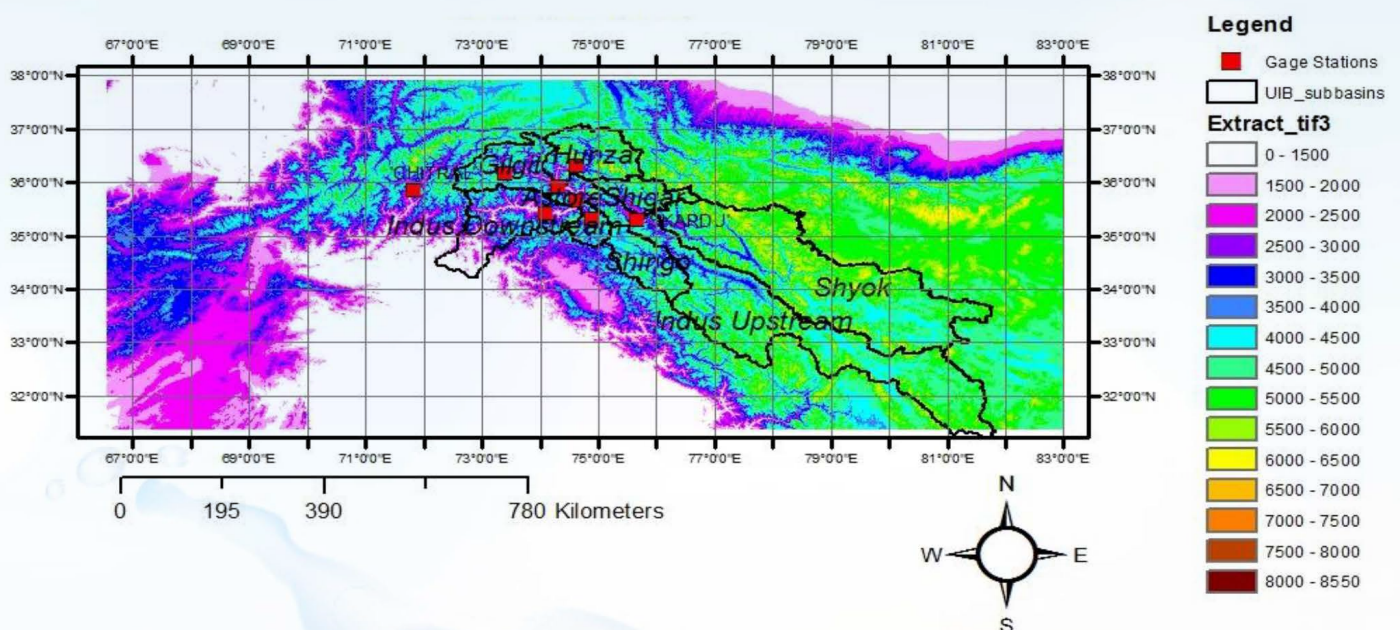
U.S.-Pakistan

Centers for Advanced Studies in Water



Changing Climate in Pakistan: Food Security and Water Management Implications

Final Report 2019



Principal Investigator:

Ghulam Hussain Dars, U.S.-Pakistan Center for Advanced Studies in Water, Mehran University of Engineering and Technology Jamshoro, Pakistan

Co-Principal Investigators:

Dr. Courtenay Strong, Department of Atmospheric Sciences, University of Utah, USA

Dr. Adam Kochanski, Department of Atmospheric Sciences, University of Utah, USA



MEHRAN UNIVERSITY
of Engineering & Technology
Jamshoro, Sindh, Pakistan



Citation

Dars, G.H., Strong, C., and Kochanski, A. (2019). Changing climate in Pakistan: Food security and water management implications. U.S.-Pakistan Center for Advanced Studies in Water (USPCAS-W), MUET, Jamshoro, Pakistan

© All rights reserved by USPCAS-W. The authors encourage fair use of this material for non-commercial purposes with proper citation.

Authors

1. Ghulam Hussain Dars, U.S.-Pakistan Center for Advanced Studies in Water, Mehran University of Engineering and Technology Jamshoro, Pakistan
2. Dr. Courtenay Strong, Department of Atmospheric Sciences, University of Utah, USA
3. Dr. Adam Kochanski, Department of Atmospheric Sciences, University of Utah, USA

ISBN

978-969-23238-6-4

Acknowledgment

This work was made possible by the support of the United States Government and the American people through the United States Agency for International Development (USAID).

Disclaimer

The contents of the report are the sole responsibility of the authors and do not necessarily reflect the views of the funding agency and the institutions they work for.



USAID
FROM THE AMERICAN PEOPLE

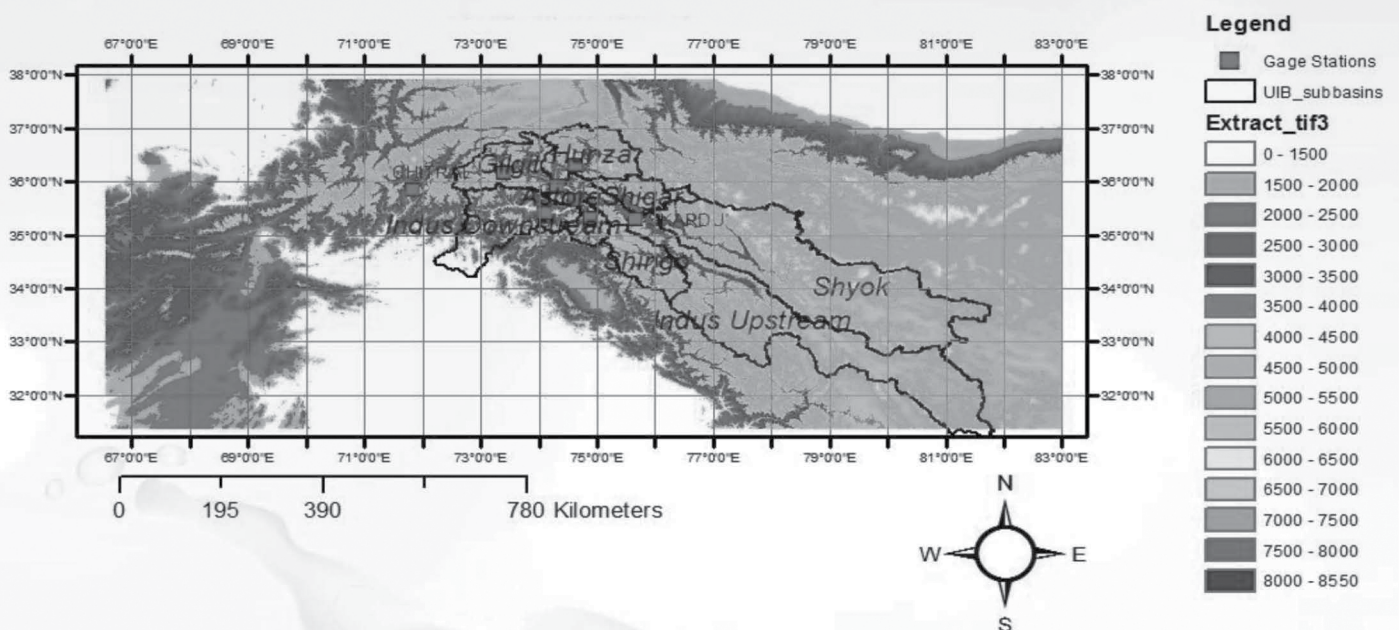
U.S.-Pakistan

Centers for Advanced Studies in Water



Changing Climate in Pakistan: Food Security and Water Management Implications

Final Report 2019



Principal Investigator:

**Ghulam Hussain Dars, U.S.-Pakistan Center for Advanced Studies in Water,
Mehran University of Engineering and Technology Jamshoro, Pakistan**

Co-Principal Investigators:

**Dr. Courtenay Strong, Department of Atmospheric Sciences,
University of Utah, USA**

**Dr. Adam Kochanski, Department of Atmospheric Sciences,
University of Utah, USA**



MEHRAN UNIVERSITY
of Engineering & Technology
Jamshoro, Sindh, Pakistan



TABLE OF CONTENTS

LIST OF ABBREVIATIONS	VI
ACKNOWLEDGMENTS	VII
EXECUTIVE SUMMARY.....	VIII
1. INTRODUCTION	1
1.1 Background.....	1
1.2 Research Hypothesis	3
1.3 Research Objectives:	3
2. MATERIALS AND METHODS	4
2.1 Study Area	4
2.2 WRF Historic Simulations	4
2.3 Model Validation	7
2.4 Trend Analysis.....	8
3. RESULTS AND DISCUSSION	9
3.1 Precipitation.....	9
3.1.1 Stations averaged precipitation trends	9
3.1.2 Domain averaged precipitation trends	13
3.2 Stations Averaged Temperature Trends	13
3.3 Discussion.....	19
3.4 Research Ouput	20
3.4.1 Research papers published	20
3.4.2 Building research partnerships.....	20
4. CONCLUSION AND RECOMMENDATIONS	21
4.1 Conclusion	21
4.2 Recommendations	21
REFERENCES	23

LIST OF TABLES

Table 2.1	Model strategy	6
Table 2.2	PMD stations, their locations, elevation and the respective domains.	7
Table 3.1.	Mean RMSE (mm), percentage difference (%) and Pearson correlation coefficient (r) of the precipitation data between WRF, gauge stations and TRMM at Skardu Station in d01, d02 and d03 domains	12
Table 3.2.	PMD stations, and the interpolated 2-m air temperature (T2) with lapse rate correction.	17
Table 3.3.	RMSE (°C) and mean bias (°C) of 2-m air temperature between WRF and the seven stations in d01 with lapse rate correction	18
Table 3.4.	Mean RMSE (°C), mean bias (°C) and Pearson correlation coefficient (r) of 2-m air temperature between WRF and station data at Skardu in the domain-01 (d01), domain-02 (d02) and domain-03 (d03) with lapse rate correction.	19

LIST OF FIGURES

Fig. 2.1:	Three domains (d01, d02 and d03) showing the locations of PMD stations. . . .	5
Fig. 3.1:	Time series comparisons between WRF (red), TRMM (green), and mean of PMD Stations (“Observed”; blue) for domain-01 (d01) (left column), domain-02 (d02) (middle column), and domain-03 (d03) (right column).	10
Fig. 3.2:	Time series comparisons of precipitation between WRF (red), TRMM (green), and gauge precipitation at Skardu station (“Observed”; blue) in d01 (left column), d02 (middle column), and d03 (right column).	11
Fig. 3.3:	Average PBIAS (%) of precipitation between WRF and mean of six stations in d01 (red) and d02 (blue).	13
Fig. 3.4:	Domain-averaged precipitation for WRF (red) and TRMM (blue) of d01 (left column), d02 (middle column), and d03 (right column).	14
Fig. 3.5:	Time series comparisons of temperature (T2 – 2 m air temperature) between WRF (red) and mean of PMD Stations (blue) for d01 (left column), d02 (middle column), d03 (right column) without any lapse rate correction.	15
Fig. 3.6:	Lapse rate between T (Kelvin) and height (m) in d01 (a), d02 (b) and d03 (c).	15
Fig. 3.7:	Time series comparisons of temperature (T2) between WRF (red) and station (“Observed”; blue) at Skardu station in d01 (left column), d02 (middle column), and d03 (right column) with lapse rate correction.	16

LIST OF ANNEXURES

Annexure A:	Seasonal precipitation trends at each station in d01, d02 and d03	28
Fig. A1:	Time series comparisons of precipitation between WRF, gauge and TRMM data at Astore station in domain-01 (d01).	28
Fig. A2:	Time series comparisons of precipitation between WRF, gauge and TRMM data at Bunji station in domain-01 (d01).	28
Fig. A3:	Time series comparisons of precipitation between WRF, gauge and TRMM data at Chillas station in domain-01 (d01).	29
Fig. A4:	Time series comparisons of precipitation between WRF, gauge and TRMM data at Chitral station in domain-01 (d01).	29
Fig. A5:	Time series comparisons of precipitation between WRF, TRMM at Gilgit station in domain-01 (d01).	30
Fig. A6:	Time series comparisons of precipitation between WRF, gauge and TRMM data at Gupis station in domain-01 (d01).	30
Fig. A7:	Time series comparisons of precipitation between WRF, gauge and TRMM data at Skardu station in domain-01 (d01).	31
Fig. A8:	Time series comparisons of precipitation between WRF, gauge and TRMM data at Astore station in domain-02 (d02).	31
Fig. A9:	Time series comparisons of precipitation between WRF, gauge and TRMM data at Bunji station in domain-02 (d02).	32
Fig. A10:	Time series comparisons of precipitation between WRF, gauge and TRMM data at Chillas station in domain-02 (d02).	32
Fig. A11:	Time series comparisons of precipitation between WRF, gauge and TRMM data at Gilgit station in domain-02 (d02).	33
Fig. A12:	Time series comparisons of precipitation between WRF, gauge and TRMM data at Gupis station in domain-02 (d02).	33
Fig. A13:	Time series comparisons of precipitation between WRF, gauge and TRMM data at Skardu station in domain-02 (d02).	34
Fig. A14:	Time series comparisons of precipitation between WRF, gauge and TRMM data at Skardu station in domain-03 (d03).	34

Annexure B:	Year-wise precipitation trends at each station in d01, d02 and d03	35
Fig. B1:	Time series of precipitation comparisons between WRF, gauge and TRMM at Astore from 1998 to 2008 in d01.	35
Fig. B2:	Time series comparisons of precipitation between WRF, Gauge and TRMM at Bunji from 1998 to 2008 in d01.	36
Fig. B3:	Time series comparisons of precipitation between WRF, Gauge and TRMM at Chillas from 1998 to 2008 in d01.	37
Fig. B4:	Time series comparisons of precipitation between WRF, Gauge and TRMM at Chitral from 1998 to 2008 in d01.	38
Fig. B5:	Time series comparisons of precipitation between WRF, Gauge and TRMM at Gilgit from 1998 to 2008 in d01.	39
Fig. B6:	Time series comparisons of precipitation between WRF, Gauge and TRMM at Gupis from 1998 to 2008 in d01.	40
Fig. B7:	Time series comparisons of precipitation between WRF, Gauge and TRMM at Skardu from 1998 to 2008 in d01.	41
Annexure C:	Spatial yearly precipitation bias in d01, d02 and d03 from 1998-2008.	42
Fig. C1:	Annual precipitation bias from 1998 through 2008 in all three domains.	42
Annexure D:	Spatial yearly precipitation bias in d01, d02 and d03 for four simulations	43
Fig. D1:	Top row is simulation-1, second row is simulation-2, third row is simulation-3 and bottom row is simulation-4.	43

LIST OF ABBREVIATIONS

CMIP5	Climate Model Inter-comparison Project Phase 5
DJF	December January February
GCM	Global Climate Model / Global Circulation Model
IPCC-AR	Intergovernmental Panel on Climate Change Assessment Report
IRB	Indus River Basin
JJA	June July August
LSM	Land Surface Model
MAM	March April May
MP	Micro-physics scheme
NCAR	National Center for Atmospheric Research
RCP	Representative Concentration Pathway
SON	September October November
TRMM	Tropical Rainfall Measuring Mission
UIB	Upper Indus Basin
W/m ²	Watts per square meter
WRF	Weather Research and Forecasting Model

ACKNOWLEDGMENTS

The U.S.-Pakistan Center for Advanced Studies in Water (USPCAS-W), Mehran University of Engineering & Technology, Jamshoro, Pakistan, is gratefully acknowledged for providing financial support for this study under its applied policy research grants program. Moreover, we would like to thank the Pakistan Meteorological Department (PMD), Karachi for their kind support and providing meteorological data. In addition, the support and resources from the Center for High-Performance Computing at the University of Utah is gratefully acknowledged.

We would also like to thank the Center authorities for extending administrative support and facilitation for implementing the project plans and successful completion of the project. Furthermore, the support, encouragement, and inspiration of Dr. Kazi Suleman Memon, Manager Research, USPCAS-W, Mehran University of Engineering and Technology, Jamshoro during report write up and reviewing it is highly acknowledged. Lastly, we are thankful to Muzafar Ali Joyo, Graphic Designer, for composing and designing this report.

EXECUTIVE SUMMARY

Investigating the trends in the major climatic variables over the Upper Indus Basin (UIB) region is difficult for many reasons, which includes highly complex terrain with heterogeneous spatial precipitation patterns, and scarcity of the gauge stations. The main objective of the study was to apply the Weather Research and Forecasting (WRF) model to simulate the spatio-temporal variability of precipitation and temperature over the UIB from 1998 through 2008 with boundary conditions derived from the Climate Forecast System Reanalysis (CFSR) data. The WRF model was configured with three nested domains (d01, d02 and d03) with horizontal resolutions increasing inward from 18 km through 6 km to 2 km grid cell resolution, respectively. Each year was simulated as a single calendar year. The simulations were then compared with the tropical rainfall measuring mission (TRMM) and PMD gauge stations data for the same time period using root mean square error (RMSE), percentage bias (PBIAS), mean bias error (MBE), and Pearson's correlation coefficient. The Mann-Kendall (MK) significance test was used to analyze the statistical significance of trends in all datasets. The results show that most of the precipitation and temperature trends in WRF, TRMM, and station data are not statistically significant. Moreover, the precipitation simulations are largely improved from d01 to d02, but not in d03. WRF tends to underestimate temperature in d01 but overestimates it in d02 and d03 after lapse rate corrections. This study presents high-resolution climatological datasets, which could be useful for climate change and other hydrological studies in this region

Keywords: WRF-ARW model; Upper Indus Basin; Karakoram Region; Pakistan; climate change

1. INTRODUCTION

1.1 Background

The Himalaya-Karakoram-Hindukush (HKH) region has got significant strategic importance due to having large amounts of snow and glacial ice (Soncini *et al.*, 2014). Often referred to as earth's "third pole" (Farhan *et al.*, 2015) (to indicate its massive ice and snow storage comparable to the North and South poles), it provides freshwater supply for agriculture, energy production, and drinking purposes to 1.5 billion people living in its catchments (Immerzeel *et al.*, 2010). The HKH region is also hydrologically important due to the presence of major rivers such as the Indus, Ganges, and Brahmaputra in it.

Indus Basin Irrigation System (IBIS) is one of the largest irrigation systems in the world, which not only supports over 90% of Pakistan's agricultural production (Immerzeel *et al.*, 2010), but also contributes to majority of the water needs of the country. Over the catchment area up to the Tarbela Reservoir (known as UIB), the contribution from snow and glacier melt runoffs accounts for about 70-80%, and Karakoram Mountains alone contribute to more than 50% of runoff (Immerzeel *et al.* 2010). Despite the hydrological importance, there is no consensus in the assessment of the stability of the glaciers in the region. Previous studies have shown conflicting results for glaciers located in the Karakoram ranges, concluding that they are stable, retreating or even advancing (so called Karakoram Anomaly (Hewitt 2005; Shafique *et al.*, 2018).

The Indus River Basin (IRB) has experienced increasing temperatures and features immense spatial variability in climate (Chaudhary *et al.*, 2009). The northern parts of the Indus River consist of high mountains, including the HKH mountain ranges, whereas its southern parts consist of flat plains. The climate in the northern parts (UIB) is largely influenced by western disturbances, and this region receives most of the precipitation (i.e. up to 2000 mm) in the winter season (Dimri *et al.*, 2015). However, the precipitation in the Lower Indus Basin (LIB, southern parts) is driven by the monsoon precipitation in the summer season, which ranges from 100 to 500 mm (Frenken 2011). In the Indus Basin, the mean monthly temperature varies from 2 to 49 °C (Frenken 2011).

As Indus River is largely dependent on the cryosphere melt, it has become highly vulnerable to climate (Mahessar *et al.*, 2017). Global Climate Risk Index (CRI) 2018 (Eckstein *et al.* 2017) has placed Pakistan in the top ten countries that are most affected by climate change. Global climate models (GCMs) are the basic tools to simulate and project climate change, but their low spatial resolution makes them unable to resolve mesoscale flow patterns (Immerzeel and Bierkens 2012). Several

studies (Kazmi *et al.*, 2015; Su *et al.*, 2016; Amin *et al.*, 2018) have downscaled GCM simulations over the IRB (for example, (Kazmi *et al.*, 2015; Su *et al.*, 2016; Amin *et al.*, 2018)), and found that temperature will continue to increase, but precipitation will be highly uncertain over this region. In addition, GCMs do not have the capability to resolve the orographic precipitation in complex mountainous regions such as UIB. This uncertainty in projected changes in climatic variables, especially precipitation, causes substantial uncertainty in runoff estimations.

In addition, the UIB is a data-scarce region where very few rain gauges are installed. These gauges are unevenly distributed and primarily at low-elevation valley locations, raising concerns about their representativeness of higher elevation orographic effects (Maussion *et al.*, 2014). The lack of sufficient meteorological observations is usually very challenging for flood forecasting and water resource management over this region. Complex topography, coupled with challenges of field study in this region, has led to considerable uncertainty in assessing glacial mass balance and even meteorological trends. Moreover, the available global reanalysis datasets are useful to assess the large scale flow patterns over this region, but their coarse resolution cannot effectively characterize the complex orography and other local dynamics (Maussion *et al.*, 2014; Norris *et al.*, 2017).

Regional climate models such as Advanced Research Weather Research & Forecasting model (ARW-WRF, hereafter WRF) can be applied to simulate climatic parameters in complex terrain at high resolution. High-resolution atmospheric modeling can fill the gap of observational data scarcity to advance the understanding of atmospheric variability. The WRF model has successfully been applied worldwide (Sato 2013; Collier and Immerzeel 2015; Scalzitti *et al.*, 2016b, a; Sikder and Hossain 2016), and to the Tibetan Plateau (Li *et al.*, 2009; Maussion *et al.*, 2011; Gao *et al.*, 2015; Viterbo *et al.*, 2016; Norris *et al.*, 2018). Gao *et al.* (2015) applied the WRF model to perform 32 years (1979–2011) of simulations over the Tibetan Plateau at 30 km grid cell resolution, but this resolution is still somewhat coarse for capturing orographic precipitation patterns (Norris *et al.*, 2018). Maussion *et al.* (2014) also used the WRF model to perform 11 years (October 2000 – September 2011) simulations over the Tibetan Plateau at 30 km and 10 km grid cell resolution in the outer and inner domain, respectively. Norris *et al.* (2017) have emphasized the importance of finer grid cell resolution (2 km or less) over this region to simulate climatic variables, especially precipitation. However, investigating the long-term high-resolution meteorological variability (at 2 km) over the Karakoram Mountain Range is lacking, which is very important for the glaciological and hydrological communities.

In view of the above, we have used the WRF model version 3.8.1 (Skamarock *et al.* 2008) to dynamically downscale 11 years (1998-2008) over the UIB, focusing on

the Central Karakoram Region in the inner domain at 2 km resolution. Our purpose in this study is to investigate spatiotemporal variability in climate over this region, and to assess the ability of WRF to capture observed variations using an analysis of correlation, bias, and trend. The WRF model has been configured with three nested domains (d01-d03) with the boundary conditions derived from the National Oceanic and Atmospheric Administration (NOAA)'s National Center of Environmental Prediction (NCEP) 6-hourly Climate Forecast System Reanalysis (CFSR) data (Saha *et al.*, 2010), which has 38-km horizontal resolution. This study provides an analysis of the WRF model's applicability over the complex terrain of the UIB at annual as well as seasonal scale.

1.2 Research Hypothesis

High-resolution dynamical downscaling methods perform better than statistical downscaling methods in complex terrain such as mountainous region of the UIB, and are capable of capturing orographic precipitation (Norris *et al.*, 2017).

1.3 Research Objectives:

- i. To simulate major hydro-climate variables (precipitation and temperature) using a high-resolution dynamical downscaling model [Weather Research and Forecasting (WRF) model];
- ii. To test whether the WRF model can accurately simulate hydro-climate patterns over complex terrain;

2. MATERIALS AND METHODS

2.1 Study Area

This study has three domains with different scales and grid cell resolutions. The inner domain (d03), ranging from 35.187 °N to 36.122 °N latitude and 75.19 °E to 77.273 °E longitude, covers an area of 19,702 km². The study area is localized on the Central Karakoram Region. The middle domain (d02) ranges from 34.292 °N to 37.073 °N latitude and 73.109 °E to 79.483 °E longitude and covers an area of 170,748 km². It focuses on the Karakoram Mountain Range, i.e., Hunza, Shigar, and large portion of Shyok River Basin (Fig. 2.1). The outer domain (d01) ranges from 31.373 °N to 39.870 °N latitude and 66.560 °E to 86.240 °E longitude and covers an area of 1,490,400 km². The elevation of this study region varies from 135 to 8550 m above sea level, which has been derived from a 90 m resolution digital elevation model (DEM) from the Shuttle Radar Topography Mission (SRTM) project. The Karakoram Range is a high altitude, complex mountainous area with the Hindu Kush and Himalayan Mountains located on its west and east, respectively. Typically, three major factors may influence the climate over the Karakoram region: the winter westerlies, the summer monsoon, and a high-pressure system formed over high Asia (Hewitt 2014). Most of the precipitation over this region occurs in winter and spring and is influenced by winter westerly flow (Pritchard *et al.*, 2019). As the region of interest hosts more than 7000 glaciers, which are about 20% of the total glaciers located in the Greater Himalayan Region (Hewitt 2014), its climate is of vital importance for the people relying on the glacier melt as a sustainable water supply.

2.2 WRF Historic Simulations

The Advanced Research Weather Research & Forecasting model (ARW-WRF, hereafter WRF) version 3.8.1 (Skamarock *et al.*, 2008) was used to dynamically downscale 11 years' (1998-2008) CFSR data (Saha *et al.*, 2010), which has approximately 38-km horizontal grid resolution. Each year was simulated as a single calendar year starting from 1 January at 00 hours and 00 minutes to 31 December at 23 hours and 59 minutes. The motivation for using CFSR data in this study has been taken from Bao and Zhang (2013), wherein they evaluated several datasets over Tibetan Plateau. They found that the CFSR and the Interim European Center for Medium-Range Weather Forecasts (ECMWF) reanalysis datasets (ERA-Interim) can simulate atmospheric changes effectively. They showed that both datasets presented smaller root mean square (RMS) error and mean bias. The main reason for selecting the CFSR dataset, specifically in this study, was its resolution. The CFSR dataset has a higher spatial resolution (0.5° by 0.5°) than ERA-Interim (0.75° by 0.75°).

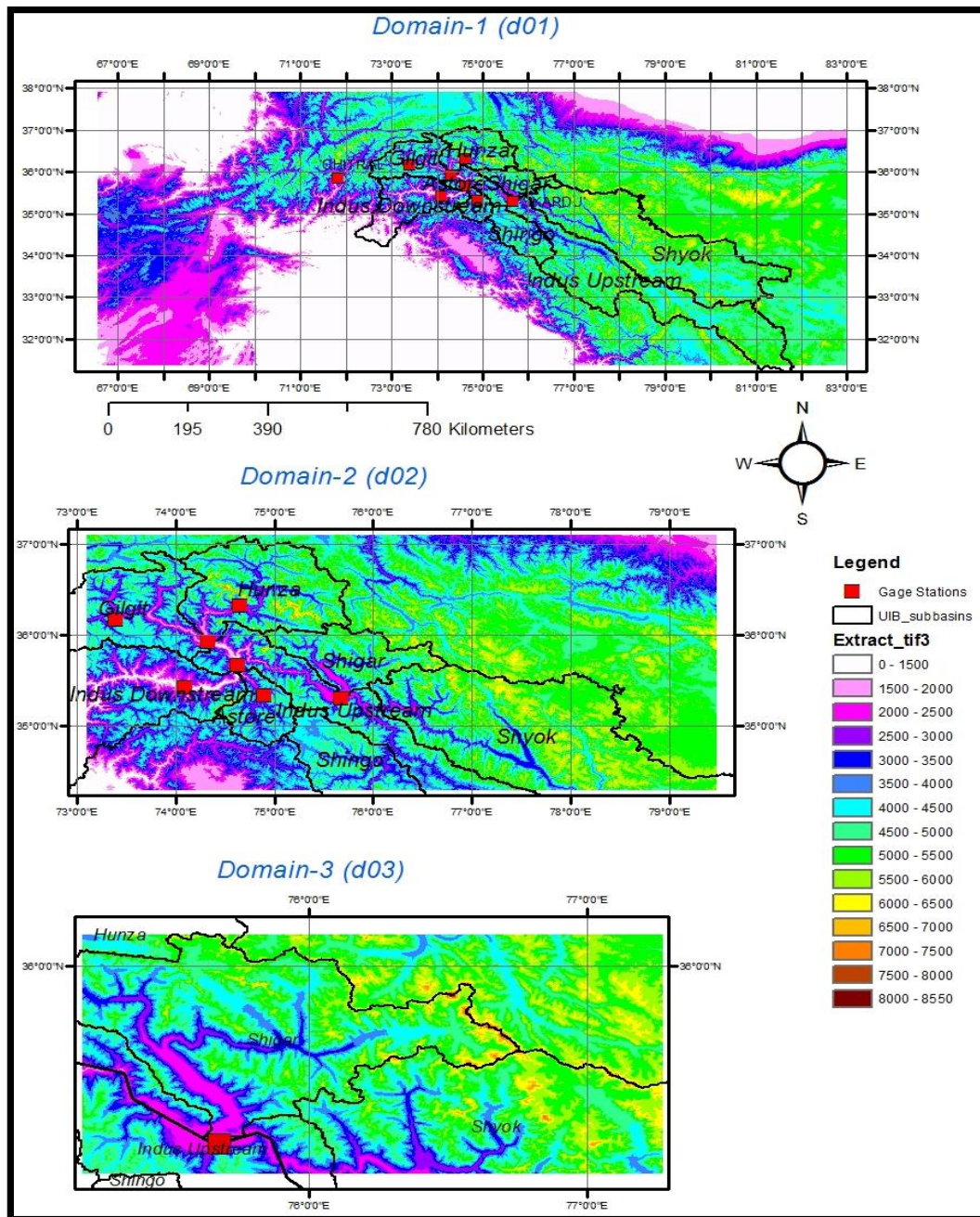


Fig. 2.1: Three domains (d01, d02 and d03) showing the locations of PMD stations
 The WRF model used in this study is configured with three nested domains with gradually increasing horizontal resolution from 18 km through 6 km to convection-permitting 2 km, so that the innermost domain does not rely on a cumulus parameterization. The model configuration presented in Fig. 2.1 was specifically chosen to limit the influence of boundary conditions on the results by assuring large margins between the nested domains. In addition, the relaxation zone of five points used in this study is very small compared to the domain sizes. The choice of the innermost domain size stems from the work by Norris *et al.* (2017) who have emphasized that a grid cell resolution of 2-km or finer is required to resolve orographic precipitation in this region. The detailed model strategy and parameterization schemes used in this study are given in Table 2.1.

Table 2.1 Model strategy

A. Physical parameterization schemes	
Land surface model (LSM)	Noah multi-parameterization (Noah-MP) (Niu <i>et al.</i> 2011)
Planetary boundary layer (PBL)	Yonsei University (YSU) scheme (Hong <i>et al.</i> 2006)
Microphysics	Thompson microphysics scheme (Thompson <i>et al.</i> 2008)
Longwave radiation	Rapid radiative transfer model (RRTM) (Iacono <i>et al.</i> 2008)
Shortwave radiation	Dudhia scheme (Dudhia 1989)
Land surface	Revised MM5 scheme (Monin and Obukhov 1954)
Cumulus parameterization	Betts-Miller-Janjic scheme (Janjić 2000) in d01 and d02
B. Grids and Nesting Strategy	
Nesting	Two-way Nesting; Nested in a cascade approach (d01-d02-d03)
Horizontal grid cell resolution	18km, 6km, and 2km
Map projection	Lambert conformal
Number of vertical layers	30
Top-level pressure	5000 Pa
Center point of domains	35.80°N, 76.40°E
Timestep	Parent time step ratio of 1:3 40s in d01, 13.3s in d02, and 4.44s in d03
C. Sensitivity Analysis	
Simulation - 1	Thompson and Noah-MP
Simulation - 2	Morrison and Noah-MP
Simulation - 3	Goddard and Noah-MP
Simulation - 4	Thompson and CLM4

Research shows that WRF is highly sensitive to the selection of the land surface model (LSM) and cloud microphysical scheme (Norris *et al.* 2017). Based on limited computational resources, four simulation experiments (Table 2.1, Section-C) were performed for the year 2004 with a combination of three cloud microphysical schemes (Thompson, Morrison, and Goddard), and two land surface models (Noah-MP and CLM4). The RMS error and Pearson's r between WRF, stations, and Tropical Rainfall Measuring Mission (TRMM) data were estimated at Skardu station for the year 2004. The results showed that the RMS error between the WRF and station data is lower in all three domains in the simulation-1. In addition, Pearson's r between the WRF and station data in the simulation-1 is slightly higher than the other three simulations. Therefore, the results suggested that out of the tested configuration, simulation-1 (Thompson and Noah-MP) offered the best performance. This is also consistent with (Norris *et al.* 2017), wherein they performed sensitivity analysis over the same region for selected summer and winter days.

2.3 Model Validation

We evaluated the WRF temperature and precipitation output with the Pakistan Meteorological Department (PMD) meteorological data. PMD operates only seven stations in the region of interest above Tarbela Reservoir (Table 2.2).

Table 2.2 PMD stations, their locations, elevation and the respective domains

S. No.	Station	Lon	Lat	Elevation (m)	Domain(s)
1	Chilas	74° 06'	35° 25'	1250	d01, d02
2	Bunji	74° 38'	35° 40'	1372	d01, d02
3	Gupis	73° 24'	36° 10'	2156	d01, d02
4	Skardu	75° 41'	35° 18'	2317	d01, d02,d03
5	Astore	74° 54'	35° 20'	2168	d01, d02
6	Gilgit	74° 20'	35° 55'	1460	d01, d02
7	Chitral	71° 50'	35° 51'	1497	d01

Because of the limited availability of station data, we also assessed the WRF precipitation output with the TRMM 3B42V7 gridded precipitation data (Huffman *et al.*, 2007) at monthly temporal scale. The TRMM data are available on a 0.25° by 0.25° latitude-longitude grid at 3-hourly temporal resolution. TRMM data are collected from remote sensing and adjusted based on the monthly gauge data. Despite its coarse resolution and other limitations, TRMM 3B42V7 is considered to be one of the reliable gridded precipitation dataset (Norris *et al.*, 2017; Krakauer *et al.*, 2019). Krakauer *et al.* (2019) compared different precipitation datasets with the available stations

data over the Indus Basin and found the TRMM dataset performing best among the remote sensing datasets. Similarly, Ali *et al.* (2017) evaluated the TRMM Multisatellite Precipitation Analysis (TMPA) precipitation products (3B42V6, 3B42V7, and 3B42RT) with gauge stations over the Hunza Basin in Karakoram Mountainous range. They also found 3B42V7 reasonably better than the other two products. Several studies (Maussion *et al.*, 2014; Norris *et al.*, 2017) have also evaluated the WRF precipitation with the TRMM dataset (for example, (Maussion *et al.*, 2014; Norris *et al.*, 2017)).

The WRF precipitation output is evaluated by RMSE, percentage bias, and Pearson correlation coefficient (r), whereas WRF temperature output is evaluated by RMSE, mean bias, and Pearson correlation coefficient. The expressions of RMSE, percentage bias (PBIAS), and mean bias for n grid points or n stations are:

$$RMSE = \sqrt{\frac{1}{n} \sum_{i=1}^n (M_i - O_i)^2}, \quad (1)$$

$$PBIAS = \frac{1}{n} \sum_{i=1}^n ((M_i - O_i) / O_i) * 100, \quad (2)$$

$$Mean\ bias = \frac{1}{n} \sum_{i=1}^n (M_i - O_i), \quad (3)$$

where M and O represent model simulations and observed data, respectively.

2.4 Trend Analysis

In this study, we have performed a trend analysis using the Mann-Kendall (MK) significance test (Mann, Henry 1945; Kendall 1948). It is a non-parametric test, and less affected by the extreme values, which is also widely used to detect trends in hydrologic time series (Arfan *et al.* 2019; Hu *et al.* 2019).

3. RESULTS AND DISCUSSION

In this section, we evaluate the simulated precipitation in the three domains using the PMD meteorological data and TRMM data. However, the simulated temperature is evaluated only using the PMD meteorological data.

3.1 Precipitation

3.1.1. Stations averaged precipitation trends

This section describes the extent to which WRF is accurate in reproducing the spatio-temporal variability of precipitation in the three domains of UIB. The annual and seasonal mean precipitation trends for WRF, TRMM, and stations data are shown in Fig 2. In addition, the Pearson correlation coefficient 'r' is computed between WRF and both the observed datasets.

There are seven stations (Table 2.2) in the outer domain (d01), and WRF and TRMM data are extracted at these gauge stations. When WRF, TRMM, and gauge data at these stations are averaged and compared, WRF tends to overpredict the total annual precipitation relative to TRMM and the gauge data (left column, Fig. 3.1). For seasonal precipitation variation from 1998 to 2008, WRF shows strong correlation ($r = 0.63$ or more) with TRMM and gauge precipitation for all seasons except summer, wherein WRF is positively correlated with the gauge and TRMM data but at low correlation. Similarly, WRF annual precipitation is significantly correlated with TRMM and gauge data ($p < 0.05$). However, trend analyses for WRF, TRMM, and gauge stations located in d01 do not show any statistically significant trends for either precipitation or temperature for all four seasons.

There are six gauge stations in the middle domain (d02), and WRF and TRMM data are extracted at these gauge locations. When WRF, TRMM, and gauges data at these six stations are averaged and compared, WRF underpredicts the total annual precipitation compared with the TRMM and gauge data (middle column, Fig. 3.1). In the winter season, WRF is significantly correlated with TRMM and gauge stations with $r = 0.64$ ($p=0.03$) and 0.72 ($p=0.01$), respectively. For the spring season, WRF and TRMM precipitation are significantly correlated at $r = 0.67$ ($p=0.02$), and WRF shows a positive correlation with 'r' value of 0.51 ($p=0.1$) with gauge stations. Similar to the summer season in d01, the WRF and TRMM precipitation are not significantly correlated in d02. However, WRF and gauge stations show a positive correlation of 0.57 ($p=0.07$). For the autumn season, WRF and TRMM are positively correlated at $r = 0.5$ ($p=0.1$). However, the gauge data shows no significant correlation with WRF. For average annual precipitation, WRF is significantly correlated with TRMM at $r = 0.59$ ($p=0.05$),

whereas it is not significantly correlated with gauge stations. However, trend analyses for WRF, TRMM, and gauge stations located in d02 do not show statistically significant trends for either precipitation or temperature for all four seasons.

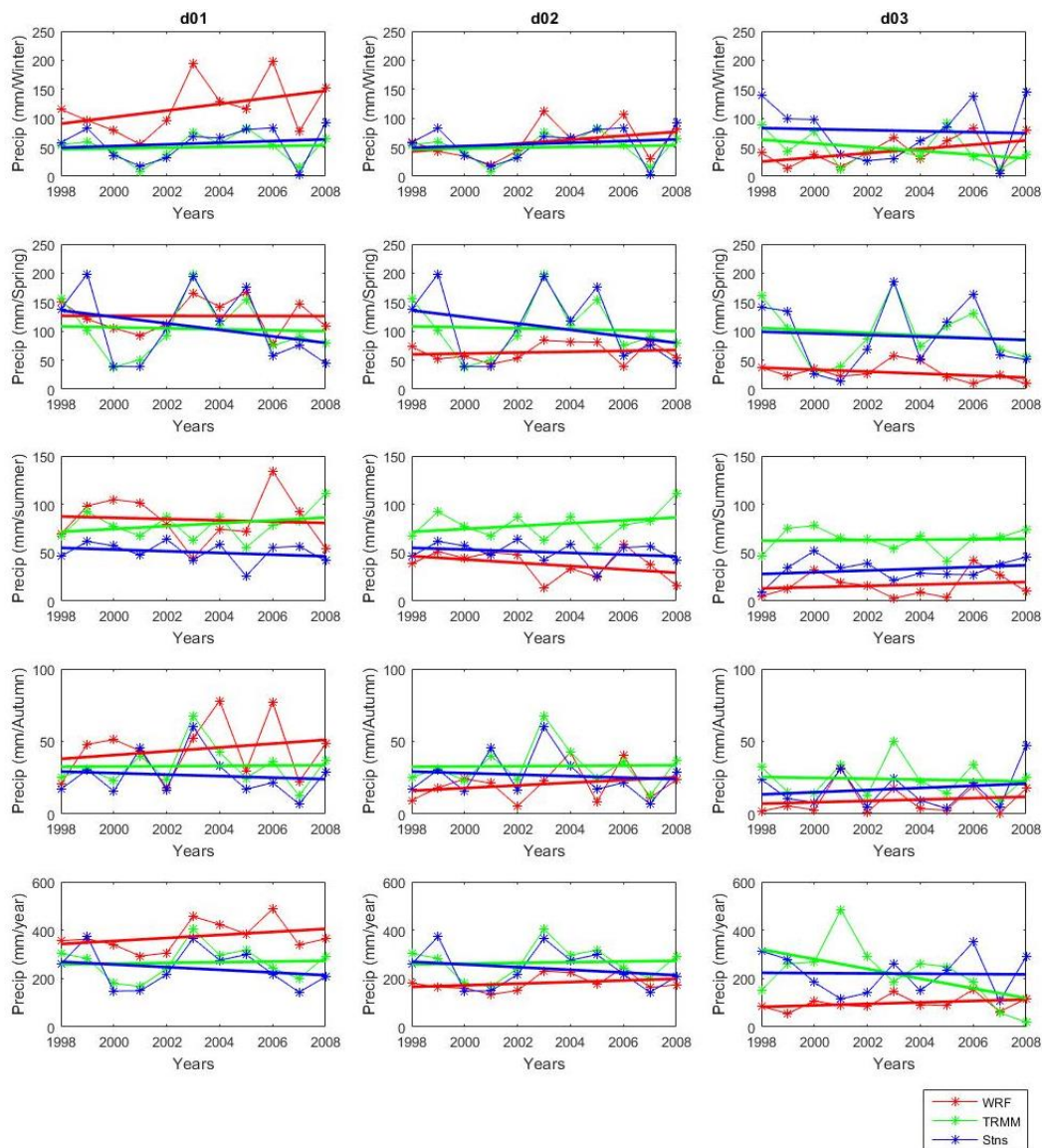


Fig. 3.1: Time series comparisons between WRF (red), TRMM (green), and mean of PMD Stations (“Observed”; blue) for domain-01 (d01) (left column), domain-02 (d02) (middle column), and domain-03 (d03) (right column). From top to bottom, the five rows correspond to winter (DJF), spring (MAM), summer (JJA), autumn (SON), and annual. The straight lines are least-square linear regressions.

There is only one gauge station in d03 located at Skardu. Comparing WRF precipitation with gauge and TRMM data at this station, WRF underpredicts the total annual precipitation (right column, Fig. 2.1). For annual precipitation, WRF is not significantly correlated with TRMM data but is positively correlated with gauge data at 0.49 ($p=0.12$). Most of these trends for precipitation and temperature are not statistically

significant. For seasonal precipitation variation, WRF shows a positive but less significant correlation with TRMM and gauge precipitations for all seasons except autumn, where WRF and gauge station show a strong positive correlation at 0.68 ($p=0.02$).

The important aspect is how the simulated precipitation amount and bias change as resolution increases. Fig. 3.2 shows how precipitation amount changes at Skardu station with the increase of resolution. The results show that the precipitation simulations are largely improved from d01 to d02. However, d02 and d03 are nearly identical in simulating precipitation, and do not show any clear improvement (Table 3.1). In addition, WRF tends to overestimate precipitation in d01, and underestimate it in d02 and d03.

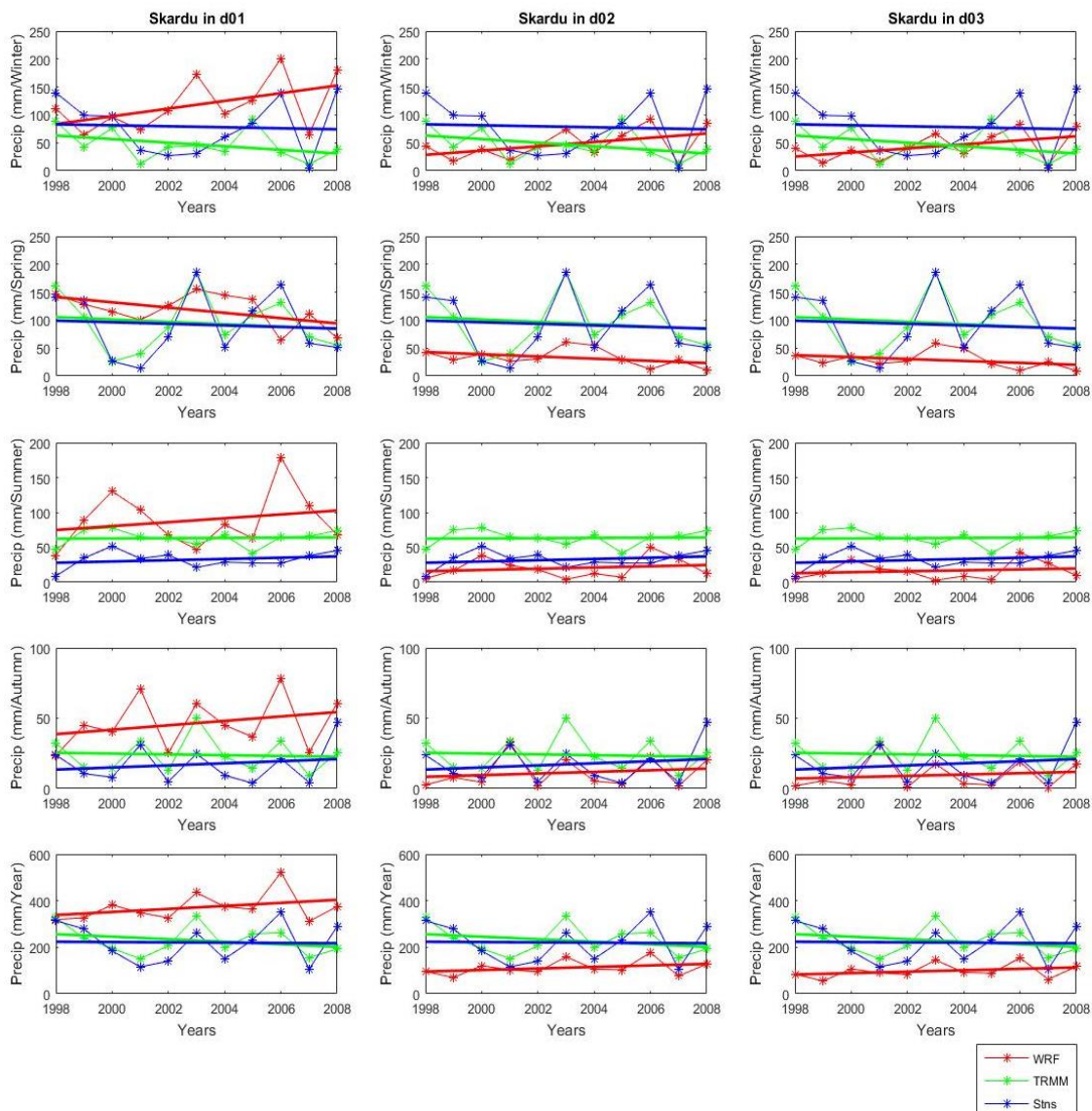


Fig. 3.2: Time series comparisons of precipitation between WRF (red), TRMM (green), and gauge precipitation at Skardu station (“Observed”; blue) in d01 (left column), d02 (middle column), and d03 (right column). From top to bottom, the five rows correspond to winter (DJF), spring (MAM), summer (JJA), autumn (SON), and annual. The straight lines are least-square linear regressions.

Table 3.1. Mean RMSE (mm), percentage difference (%) and Pearson correlation coefficient (r) of the precipitation data between WRF, gauge stations and TRMM at Skardu Station in d01, d02 and d03 domains

Season	Parameters	d01	d02	d03
Winter (DJF)	RMSE (mm) btw WRF & Station (WRF & TRMM)	62 (86)	51 (32)	53 (31)
	PBIAS (%) btw WRF & Station (WRF & TRMM)	203 (150)	-4 (-65)	-15 (-78)
	Pearson correlation coefficient (r) btw WRF & Station (WRF & TRMM)	0.11 (0.47)	0.24 (0.53)	0.28 (0.54)
Spring (MAM)	RMSE (mm) btw WRF & Station (WRF & TRMM)	62 (50)	81 (76)	84 (80)
	PBIAS (%) btw WRF & Station (WRF & TRMM)	95 (63)	-61 (-54)	-70 (-60)
	Pearson correlation coefficient (r) btw WRF & Station (WRF & TRMM)	0.42 (0.24)	0.36 (0.18)	0.36 (0.18)
Summer (JJA)	RMSE (mm) btw WRF & Station (WRF & TRMM)	67 (43)	18 (45)	20 (48)
	PBIAS (%) btw WRF & Station (WRF & TRMM)	71(38)	-161 (-69)	-172 (-75)
	Pearson correlation coefficient (r) btw WRF & Station (WRF & TRMM)	0.51 (0.51)	0.51 (0.45)	0.51 (0.44)
Autumn (SON)	RMSE (mm) btw WRF & Station (WRF & TRMM)	33 (27)	10 (16)	12 (17)
	PBIAS (%) btw WRF & Station (WRF & TRMM)	224 (117)	-123 (-58)	-139 (-67)
	Pearson correlation coefficient (r) btw WRF & Station (WRF & TRMM)	0.62 (0.61)	0.68 (0.74)	0.68 (0.74)
Annual	RMSE (mm) btw WRF & Station (WRF & TRMM)	167 (157)	129 (129)	141 (141)
	PBIAS (%) btw WRF & Station (WRF & TRMM)	79 (70)	-56 (-49)	-63 (-56)
	Pearson correlation coefficient (r) btw WRF & Station (WRF & TRMM)	0.33 (0.52)	0.40 (0.51)	0.40 (0.50)

We evaluated the PBIAS of WRF with the six stations (Table 2.2), which are located in both d01 and d02. The results (Fig. 3.3) show that the precipitation simulations are largely improved from d01 to d02. The d01 has a positive bias in all seasons, whereas d02 has a negative bias except during winter. The wet bias in the winter is broadly consistent with Norris *et al.* (Norris *et al.*, 2017, 2018). In d01, spring has the smallest PBIAS, whereas autumn has the smallest PBIAS in d02.

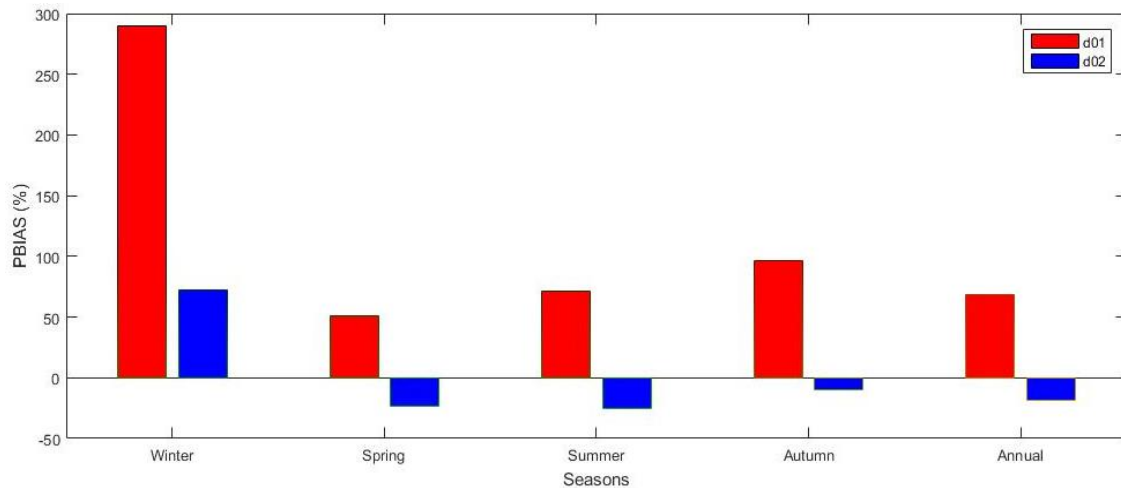


Fig. 3.3: Average PBIAS (%) of precipitation between WRF and mean of six stations in d01 (red) and d02 (blue).

3.1.2 Domain averaged precipitation trends

The domain averaged annual and seasonal precipitation plots between WRF and TRMM are shown in Fig. 3.4. The outer domain (d01), middle domain (d02), and inner domain (d03) are shown at left, middle, and right panels, respectively. In addition, the Pearson correlation coefficient ‘r’ and significance level between domain averaged WRF and TRMM precipitation are estimated. The results show that the mean WRF and TRMM data are significantly correlated ($p < 0.05$) in all seasons except summer where the correlation and significance level between the WRF and TRMM in all domains is quite low. However, the correlation and significance level between WRF and TRMM in the inner domain for winter and autumn seasons is also low. The domain averaged precipitation comparisons exhibit better agreement on inter-annual variability of precipitation than the gauge-site comparisons. However, WRF seems to overpredict the precipitation in most cases except for summer and autumn seasons in the domain 01, and summer season in the domain 03.

3.2 Stations Averaged Temperature Trends

This section examines the extent to which WRF is accurate in reproducing the spatio-temporal variability of temperature in the three domains. The WRF output is compared with the PMD station data. The annual and seasonal mean temperature plots

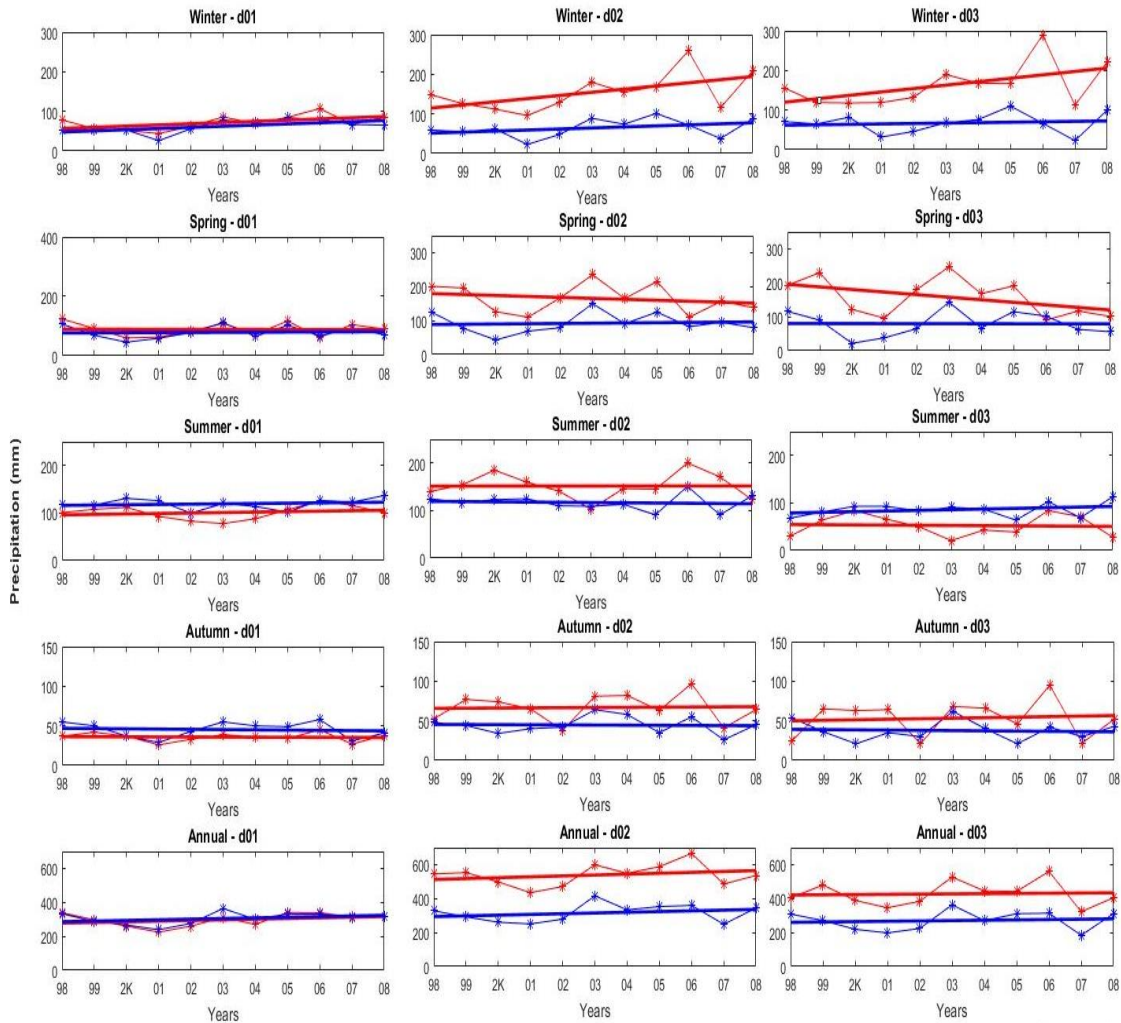


Fig. 3.4: Domain-averaged precipitation for WRF (red) and TRMM (blue) of d01 (left column), d02 (middle column), and d03 (right column).

are shown in Fig. 3.5. For all the three domains, WRF underpredicted the average annual and seasonal temperatures compared to the seven PMD stations data. In d01 and d02, the WRF data are strongly correlated with the stations data ($r = 0.72$ or more) in all seasons, except autumn in which correlation between WRF and stations data is lower but still positive. However, in d03, the WRF data are strongly correlated with the stations data in all seasons, except autumn and annual in which correlation between WRF and stations data is lower but still positive. However, most of these trends for temperature are not statistically significant except autumn, wherein the stations data in d03 shows a statistically significant trend.

Figure 3.6 shows the change in the mean lapse rate with altitude in all three domains. The average lapse rate for d01, d02, and d03 across the simulated period (1998 – 2008) is estimated to be -7.2816 , -8.0419 , and -6.7637 °C/km, respectively. These lapse rates are used to vertically interpolate the simulated temperature time series to the actual heights of the stations. For each station, the difference between the station

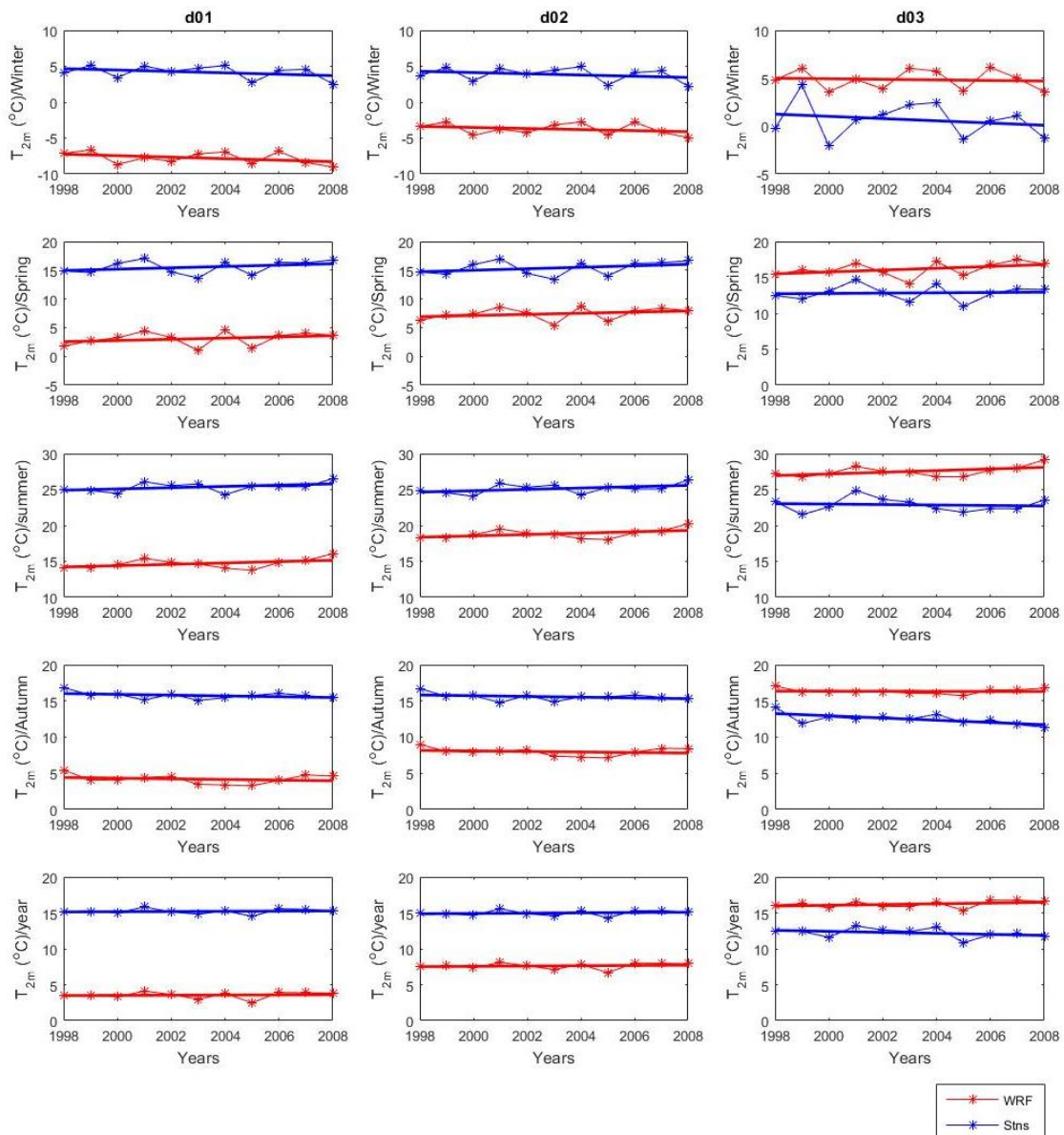


Fig. 3.5: Time series comparisons of temperature (T_2 – 2 m air temperature) between WRF (red) and mean of PMD Stations (blue) for d01 (left column), d02 (middle column), d03 (right column) without any lapse rate correction.

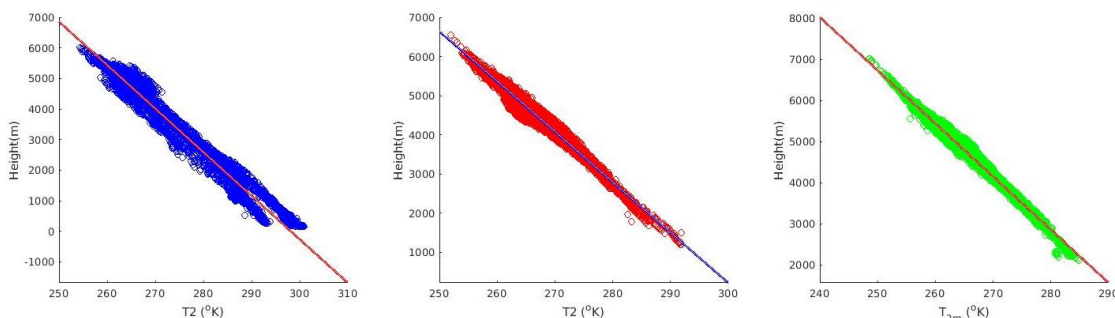


Fig. 3.6: Lapse rate between T (Kelvin) and height (m) in d01 (a), d02 (b) and d03 (c) height and WRF height is computed, multiplied by the average lapse rate, and added to the simulated temperature values (Table 3.2). There was a large cold bias in d01 (about 10°C ; Fig. 6, left column), so we present RMSE and mean bias at all stations

in d01 with lapse rate correction (Table 3.3). These results show that Bunji has the lowest, and Gupis has the highest mean bias and RMSE in all seasons.

The important feature is how the simulated temperature and bias changes as the resolution increases. Fig. 3.7 shows how temperature changes at the Skardu station with the increase of resolution, and Table 3.4 shows RMSE, mean bias, and the Pearson correlation coefficient (r) between WRF and station temperature at Skardu in all three domains after lapse rate corrections. The results show that RMSE and mean bias are noticeably changed from d01 to d03 but not improved. However, Pearson correlation coefficient is increased from d01 to d02 and is similar between d02 and d03 (Table 3.4). It shows that the WRF tends to underestimate the 2-m air temperature in d01 (annual mean bias of 1.86°C) but overestimates the 2-m air temperature in d02 (annual mean bias of 4.42°C) and d03 (annual mean bias of 3.99°C).

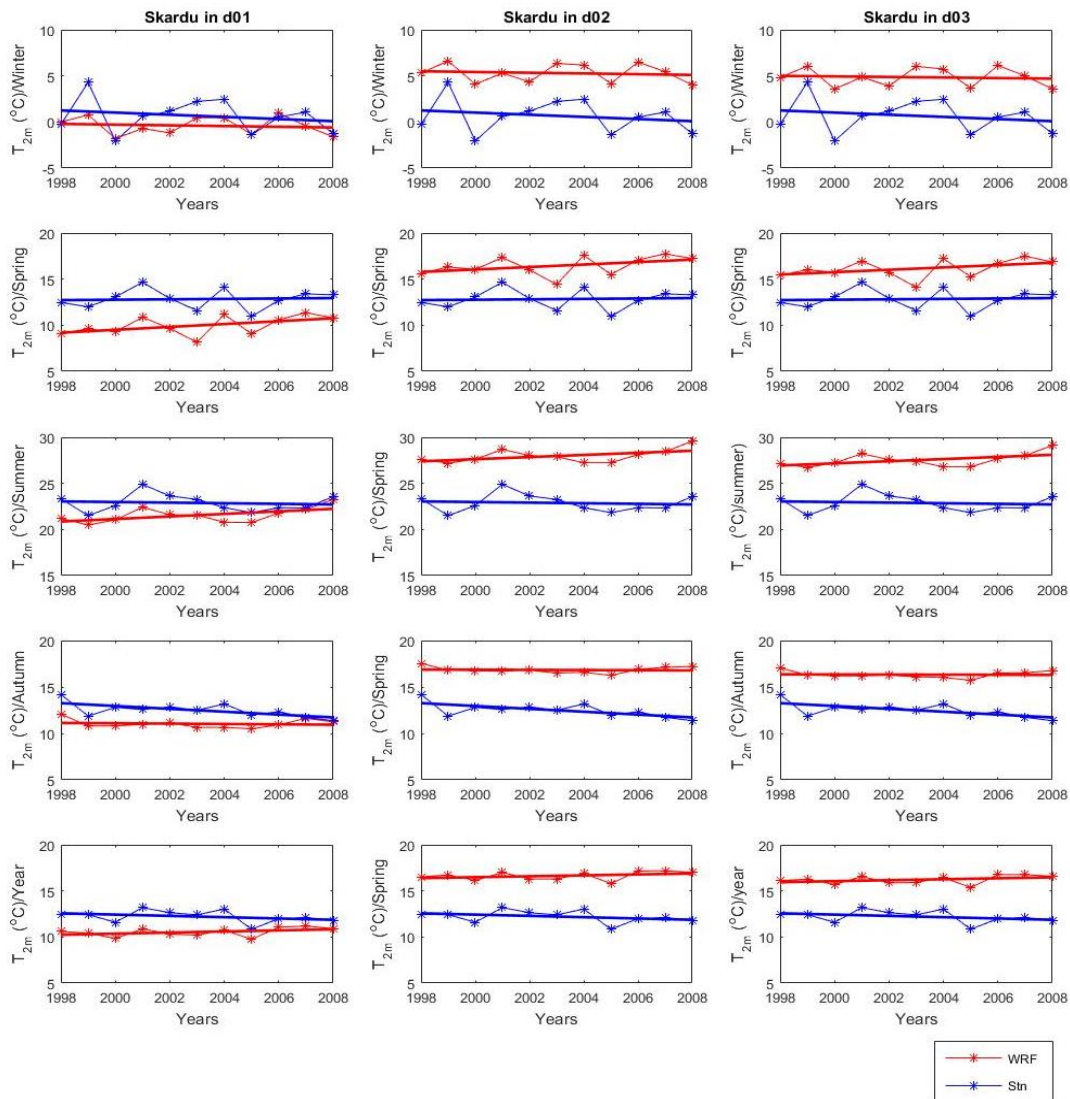


Fig. 3.7: Time series comparisons of temperature (T_2) between WRF (red) and station (“Observed”; blue) at Skardu station in d01 (left column), d02 (middle column), and d03 (right column) with lapse rate correction. From top to bottom, the five rows correspond to winter (DJF), spring (MAM), summer (JJA), autumn (SON), and annual. The straight lines are least-square linear regressions.

Table 3.2. PMD stations, and the interpolated 2-m air temperature (T2) with lapse rate correction

S. No. (1)	Station (2)	Station Elev. (m) (3)	WRF Elev. (m) (4)	Diff. (m) (col 3 – col 4 = 5)	Interpolated T2 (°C) in d01 (col 5 X Avg. Lapse rate = 6)	Interpolated T2 (°C) in d02 (col 5 X Avg. Lapse rate = 7)	Interpolated T2 (°C) in d03 (col 5 X Avg. Lapse rate = 8)
1	Chilas	1250	2238.46	-988.46	7.198	7.949	6.686
2	Bunji	1372	2349.45	-977.45	7.117	7.861	6.611
3	Gupis	2156	3881.00	-1725	12.561	13.872	11.667
4	Skardu	2317	2899.50	-582.5	4.242	4.684	3.940
5	Astore	2168	3469.00	-1301	9.473	10.463	8.800
6	Gilgit	1460	2502.35	-1042.35	7.590	8.382	7.050
7	Chitral	1497	2856.32	-1359.32	9.898	10.932	9.194
Average		1745.71	2885.15	-1139.44	8.297	9.163	7.707

Table 3.3. RMSE (°C) and mean bias (°C) of 2-m air temperature between WRF and the seven stations in d01 with lapse rate correction

Seson	Parameters	Skardu	Chillas	Bunji	Gupis	Astore	Gilgit	Chitral
Winter (DJF)	RMSE (°C)	1.64	1.69	0.98	9.19	2.01	6.01	5.24
	Mean bias (°C)	-1.07	-1.63	-0.81	-9.13	-1.74	-5.98	-5.19
Spring (MAM)	RMSE (°C)	2.94	2.30	1.61	9.35	1.95	7.28	4.38
	Mean bias (°C)	-2.86	-2.17	-1.51	-9.23	-1.86	-7.26	-4.22
Summer (JJA)	RMSE (°C)	1.52	2.95	0.58	5.24	1.00	4.63	2.26
	Mean bias (°C)	-1.33	-2.89	-0.07	-4.85	-0.68	-4.59	-2.16
Autumn (SON)	RMSE (°C)	1.63	3.30	1.17	7.55	1.93	5.17	3.07
	Mean bias (°C)	-1.46	-3.27	-0.71	-7.46	-1.87	-5.14	-2.95
Annual	RMSE (°C)	1.78	2.50	0.82	7.70	1.58	5.74	3.67
	Mean bias (°C)	-1.68	-2.48	-0.77	-7.67	-1.54	-5.74	-3.63

Table 3.4. Mean RMSE (°C), mean bias (°C) and Pearson correlation coefficient (r) of 2-m air temperature between WRF and station data at Skardu in the domain-01 (d01), domain-02 (d02) and domain-03 (d03) with lapse rate correction

Season	Statistical measure	d01	d02	d03
Winter (DJF)	RMSE (°C)	1.64	4.78	4.35
	Mean bias (°C)	-1.07	4.63	4.19
	Pearson correlation coefficient (r)	0.76	0.88	0.88
Spring (MAM)	RMSE (°C)	2.94	3.68	3.38
	Mean bias (°C)	-2.86	3.62	3.31
	Pearson correlation coefficient (r)	0.78	0.78	0.77
Summer (JJA)	RMSE (°C)	1.52	5.14	4.70
	Mean bias (°C)	-1.33	5.09	4.64
	Pearson correlation coefficient (r)	0.64	0.62	0.62
Autumn (SON)	RMSE (°C)	1.63	4.40	3.92
	Mean bias (°C)	-1.46	4.34	3.84
	Pearson correlation coefficient (r)	0.34	0.23	0.21
Annual	RMSE (°C)	1.78	4.45	4.04
	Mean bias (°C)	-1.86	4.42	3.99
	Pearson correlation coefficient (r)	0.47	0.48	0.48

3.3 Discussion

The WRF model was applied to simulate the spatio-temporal variability of precipitation and temperature over the UIB from 1998 through 2008 using boundary conditions derived from the CFSR reanalysis dataset. The WRF model was configured with three nested domains with increasing horizontal resolution moving inward from 18 km through 6 km to 2 km grid cell resolution. The inner domain (d03) focuses on the Central Karakoram region having highly complex terrain. The simulations were then compared with TRMM 3B42V7 and PMD stations data for the same time period and analyzed at annual and seasonal scales. Satellite-based products (for example TRMM 3B42V7) can be used as a potential source of observed datasets for hydro-meteorological studies in the data-scarce regions such as UIB.

We used the Mann-Kendall (MK) significance test to analyze the statistical significance of trends. We found that most of the precipitation trends in WRF, TRMM, and gauge station locations are not statistically significant. Consistent with this study, Ahmad *et al.* (Ahmad *et al.*, 2015) estimated the significance level of precipitation of the 51-year period (1961-2011) over the Swat River Basin (located over UIB) using MK and Spearman's rho statistical tests. They found that most of the annual precipitation time series had statistically non-significant trend in the Swat River Basin. In addition, Khattak *et al.* (2011) analyzed trends in the hydro-meteorological variables over the UIB from 1967 to 2005, and found significant increasing trends ($p < 0.1$) in the stream flow and mean monthly maximum temperature but no conclusive trend in precipitation and mean monthly minimum temperature in most parts of the UIB. Likewise, Norris *et al.* (Norris *et al.*, 2018) also found no significant trend in precipitation as well as temperature over the Karakorum region.

3.4 Research Ouput

3.4.1 Research papers published

One research paper titled "Spatio-temporal variability of drought in Pakistan using Standardized Precipitation Evapotranspiration Index" is published (Jamro *et al.*, 2019) in the international journal (Applied Sciences – Impact Factor 2.217).

3.4.2 Building research partnerships

This research project provided an opportunity to work in collaboration with Dr. Courtenay Strong, Associate Professor, Department of Atmospheric Science, University of Utah, and Dr. Adam Kochanski, Research Assistant Professor, Department of Atmospheric Science, University of Utah. Court, Adam and Dars have sustained this research partnership to analyze the climate change impacts on water resources using more robust tools and models. Their partnership was able to explore more funds for research over the Indus River Basin (IRB) and Pakistan. They won one research project titled "Improved hydro-meteorological forecasts under changing climate using robust model techniques".

4. CONCLUSION AND RECOMMENDATIONS

4.1 Conclusion

The precipitation simulations are significantly improved from domain d01 (18-km) to d02 (6-km), but d03 (2-km) does not show any clear improvement. The d01 has a positive bias in all seasons, but d02 has a negative bias except in winter. The gauges in the UIB in Pakistan suffer from undercatch for winter precipitation, especially snowfall which could cause a significant amount of wet bias in this season. However, precipitation occurs in the form of rain in spring and summer seasons over this region, which the rain gauges measure more accurately. This contributes to less discrepancy between WRF precipitation and station observations in the summer season. However, the correlation between WRF simulated and observed temperature is much better than that of precipitation.

The domain averaged analysis of WRF and TRMM precipitation revealed some interesting contrasts. The domain averaged WRF and TRMM data were significantly correlated ($p < 0.05$) in all seasons except in summer. The results also show that WRF tends to overestimate precipitation in d02 and d03.

The WRF model shows an underestimation of 2-m air temperature in all seasons in d01 and overestimation in d02 and d03 after lapse rate correction. WRF has a substantial cold bias in d01 relative to the weather stations, which stems largely from the seven station elevations averaging 1139 m below their nearest WRF grid points.

4.2 Recommendations

Following are the recommendations of this study:

- i. Knowing the limitations of the GCMs over the complex and rugged terrain, regional climate models are the best available tools to simulate climate change. This study does not intend to analyze the climatic processes that influence the precipitation and temperature but provides an overview of the ability of WRF to simulate spatiotemporal variability of precipitation and temperature over the UIB. However, the regional climate model studies are scarce as enough data are yet not available. Having few weather stations over the study region, we also used TRMM dataset to validate the WRF output. Therefore, it highlights the necessity of more permanent automated weather stations especially in the high-altitude areas where it is challenging to access and collect data especially in the winter season.
- ii. The domain averaged analysis of WRF and TRMM precipitation showed that the WRF was able to capture the precipitation trends in most of the

seasons, but tends to overestimate precipitation in d02 and d03, which may be an underestimation of precipitation by the observed datasets. This study presents high-resolution climatological datasets, which could be useful for climate change and other hydrological studies in this region. However, additional studies are required to be conducted for longer periods if the resources are available.

- iii. In addition, 5 grid points along the boundaries are lost for the relaxation zone, and then as a rule of thumb the model needs around 20 grid points to resolve scales at its native resolution. Therefore, the domain size should be large enough to handle this.

REFERENCES

- Ahmad I, Tang D, Wang T, et al (2015) Precipitation trends over time using Mann-Kendall and Spearman's Rho tests in Swat River basin, Pakistan. *Adv Meteorol* 2015:.. doi: 10.1155/2015/431860
- Ali AF, Xiao C, Anjum MN, et al (2017) Evaluation and comparison of TRMM multi-satellite precipitation products with reference to rain gauge observations in Hunza River basin, Karakoram Range, northern Pakistan. *Sustain* 9:1954. doi: 10.3390/su9111954
- Amin A, Iqbal J, Asghar A, Ribbe L (2018) Analysis of current and future water demands in the Upper Indus Basin under IPCC climate and socio-economic scenarios using a hydro-economic WEAP Model. *Water* 10:.. doi: 10.3390/w10050537
- Arfan M, Lund J, Hassan D, et al (2019) Assessment of spatial and temporal flow variability of the Indus River. *Resources* 8:103. doi: 10.3390/resources8020103
- Bao X, Zhang F (2013) Evaluation of NCEP-CFSR, NCEP-NCAR, ERA-Interim, and ERA-40 reanalysis datasets against independent sounding observations over the Tibetan Plateau. *J Clim* 26:206–214. doi: 10.1175/JCLI-D-12-00056.1
- Caldwell P, Chin HNS, Bader DC, Bala G (2009) Evaluation of a WRF dynamical downscaling simulation over California. *Clim Change* 95:499–521. doi: 10.1007/s10584-009-9583-5
- Chaudhary QZ, Mahmood A, Rasul G, Afzaal M (2009) *Climate Change Indicators of Pakistan*
- Collier E, Immerzeel WW (2015) High-resolution modeling of atmospheric dynamics in the Nepalese Himalaya. *J Geophys Res Atmos* 120:9882–9896. doi: 10.1002/2015JD023266. Received
- Dimri AP, Niyogi D, Barros AP, et al (2015) Western Disturbances: a review. *Rev Geophys* 53:225–246. doi: 10.1002/2014RG000460. Received
- Dudhia J (1989) Numerical Study of Convection Observed during the Winter Monsoon Experiment Using a Mesoscale Two-Dimensional Model. *J Atmos Sci* 46:3077–3107
- Eckstein D, Künzel V, Schäfer L (2017) Global climate risk index 2018: Who suffers most from Extreme weather events? Weather-related loss events in 2016 and 1997 to 2016
- Farhan S Bin, Zhang Y, Ma Y, et al (2015) Hydrological regimes under the conjunction of westerly and monsoon climates: a case investigation in the Astore Basin, Northwestern

Himalaya. *Clim Dyn* 44:3015–3032

Frenken K (2011) Irrigation in Southern and Eastern Asia in figures: Aquastat Survey - 2011 FAO Water Reports

Gao Y, Xu J, Chen D (2015) Evaluation of WRF mesoscale climate simulations over the Tibetan Plateau during 1979-2011. *J Clim* 28:2823–2841. doi: 10.1175/JCLI-D-14-00300.1

Heikkilä U, Sandvik A, Sorteberg A (2011) Dynamical downscaling of ERA-40 in complex terrain using the WRF regional climate model. *Clim Dyn* 37:1551–1564. doi: 10.1007/s00382-010-0928-6

Hewitt K (2005) The Karakoram Anomaly? Glacier Expansion and the 'Elevation Effect,' Karakoram Himalaya. *Mt Res Dev* 25:332–340. doi: 10.1659/0276-4741(2005)025[0332:tkagea]2.0.co;2

Hewitt K (2014) *Glaciers of the Karakoram Himalaya: Glacial Environments, Processes, Hazards and Resources*. Springer Berlin

Hong S-Y, Noh Y, Dudhia J (2006) A new vertical diffusion package with an explicit treatment of entrainment processes. *Mon Weather Rev* 134:2318–2341

Hu M, Sayaman T, TRY S, et al (2019) Trend analysis of hydro-climatic variables in the Kamo River Basin, Japan. *water* 11:1782. doi: 10.1007/s00704-018-2470-0

Huffman GJ, Bolvin DT, Nelkin EJ, et al (2007) The TRMM Multisatellite Precipitation Analysis (TMPA): Quasi-Global, Multiyear, Combined-Sensor Precipitation Estimates at Fine Scales. *J Hydrometeorol* 8:38–55. doi: 10.1175/JHM560.1

Iacono MJ, Delamere JS, Mlawer EJ, et al (2008) Radiative forcing by long-lived greenhouse gases: Calculations with the AER radiative transfer models. *J Geophys Res Atmos* 113:2–9

Ikeda K, Rasmussen R, Liu C, et al (2010) Simulation of seasonal snowfall over Colorado. *Atmos Res* 97:462–477. doi: 10.1016/j.atmosres.2010.04.010

Immerzeel WW, Beek LPH Van, Bierkens MFP (2010) Climate change will affect the Asian water towers. *Science* (80-) 328:1382–1385

Immerzeel WW, Bierkens MFP (2012) Asia's water balance. *Nat Geosci* 5:841–842

Jamro S, Dars GH, Ansari K, Krakauer NY (2019) Spatio-Temporal Variability of Drought in Pakistan Using Standardized Precipitation Evapotranspiration Index. *Appl Sci* 9:4588. doi: doi:10.3390/app9214588

Janjić ZI (2000) Comments on “Development and Evaluation of a Convection Scheme for Use in Climate Models.” *J Atmos Sci* 57:3686–3686

Kazmi DH, Li J, Rasul G, et al (2015) Statistical downscaling and future scenario generation of temperatures for Pakistan Region. *Theor Appl Climatol* 120:341–350. doi: 10.1007/s00704-014-1176-1

Kendall MG (1948) Rank correlation methods. Griffin, London, UK

Khan AJ, Koch M (2018) Correction and informed regionalization of precipitation data in a high mountainous region (Upper Indus Basin) and its effect on SWAT-modelled discharge. *water* 10:1557

Khan AJ, Koch M, Chinchilla KM (2018) Evaluation of Gridded Multi-Satellite Precipitation Estimation (TRMM-3B42-V7) Performance in the Upper Indus Basin (UIB). *Climate* 6:76

Khattak MS, Babel MS, Sharif M (2011) Hydro-meteorological trends in the upper Indus River basin in Pakistan. *Clim Res* 46:103–119. doi: 10.3354/cr00957

Krakauer NY, Lakhankar T, Dars GH (2019) Precipitation Trends over the Indus Basin. *Climate* 7:116. doi: 10.3390/cli7100116

Li M, Ma Y, Hu Z, et al (2009) Snow distribution over the Namco lake area of the Tibetan Plateau. *Hydrol Earth Syst Sci* 13:2023–2030. doi: 10.5194/hess-13-2023-2009

Mahessar AA, Qureshi AL, Dars GH, Solangi MA (2017) Climate change impacts on vulnerable Guddu and Sukkur Barrages in Indus River, Sindh. *Sindh Univ Res Jour* 49:137–142

Mann, Henry B (1945) Nonparametric tests against trend. *Econom J Econom Soc* 13:245–259

Maussion F, Scherer D, Finkelnburg R, et al (2011) WRF simulation of a precipitation event over the Tibetan Plateau, China - An assessment using remote sensing and ground observations. *Hydrol Earth Syst Sci* 15:1795–1817. doi: 10.5194/hess-15-1795-2011

Maussion F, Scherer D, Mölg T, et al (2014) Precipitation seasonality and variability over the Tibetan Plateau as resolved by the high Asia reanalysis. *J Clim* 27:1910–1927. doi: 10.1175/JCLI-D-13-00282.1

Monin AS, Obukhov AM (1954) Basic laws of turbulent mixing in the surface layer of the atmosphere. *Contrib Geophys Inst Acad Sci USSR* 151:e187

- Niu G-Y, Yang Z-L, Mitchell KE, et al (2011) The community Noah land surface model with multiparameterization options (Noah - MP): 1 . Model description and evaluation with local - scale measurements. *J Geophys Res* 116:1–19. doi: 10.1029/2010JD015139
- Norris J, Carvalho LMV, Jones C, et al (2017) The spatiotemporal variability of precipitation over the Himalaya: evaluation of one-year WRF model simulation. *Clim Dyn* 49:2179–2204
- Norris J, Carvalho LM V, Jones C, Cannon F (2018) Deciphering the contrasting climatic trends between the central Himalaya and Karakoram with 36 years of WRF simulations. *Clim Dyn* 52:159–180. doi: 10.1007/s00382-018-4133-3
- Palazzi E, Von Hardenberg J, Provenzale A (2013) Precipitation in the Hindu-Kush Karakoram Himalaya: Observations and future scenarios. *J Geophys Res Atmos* 118:85–100
- Pritchard DMW, Forsythe N, Fowler HJ, et al (2019) Evaluation of upper indus near-surface climate representation by WRF in the High Asia Refined Analysis. *J Hydrometeorol* 20:467–487. doi: 10.1175/JHM-D-18-0030.1
- Saha S, Moorthi S, Pan HL, et al (2010) The NCEP climate forecast system reanalysis. *Bull Am Meteorol Soc* 91:1015–1057
- Sato T (2013) Mechanism of orographic precipitation around the meghalaya plateau associated with intraseasonal oscillation and the diurnal cycle. *Mon Weather Rev* 141:2451–2466. doi: 10.1175/MWR-D-12-00321.1
- Scalzitti J, Strong C, Kochanski A (2016a) Climate change impact on the roles of temperature and precipitation in western U . S . snowpack variability. *Geophys Res Lett* 43:5361–5369. doi: 10.1002/2016GL068798.1.
- Scalzitti J, Strong C, Kochanski AK (2016b) A 26 year high-resolution dynamical downscaling over the wasatch mountains: Synoptic effects on winter precipitation performance. *J Geophys Res* 121:3224–3240. doi: 10.1002/2015JD024497
- Shafique M, Faiz B, Bacha AS, Ullah S (2018) Evaluating glacier dynamics using temporal remote sensing images: A case study of hunza valley, northern Pakistan. *Environ Earth Sci* 77:162. doi: 10.5194/isprs-archives-XLII-2-W13-1781-2019
- Sikder S, Hossain F (2016) Assesment of the weather research and forecasting model generalized parameterization schemes for advancement of precipitation forecasting in monsoon-driven river basins. *J Adv Model Earth Syst* 8:1210–1228. doi: 10.1002/2016MS000678

Skamarock WC, Klemp JB, Dudhia J, et al (2008) A Description of the Advanced Research WRF Version 3. Boulder, Colorado

Soncini A, Bocchiola D, Confortola G, et al (2014) Future Hydrological Regimes in the Upper Indus Basin: A Case Study from a High-Altitude Glacierized Catchment. *J Hydrometeorol* 16:306–326

Su B, Huang J, Gemmer M, et al (2016) Statistical downscaling of CMIP5 multi-model ensemble for projected changes of climate in the Indus River Basin. *Atmos Res* 178–179:138–149. doi: 10.1016/j.atmosres.2016.03.023

Thompson G, Field PR, Rasmussen RM, Hall WD (2008) Explicit Forecasts of Winter Precipitation Using an Improved Bulk Microphysics Scheme. Part II: Implementation of a New Snow Parameterization. *Mon Weather Rev* 136:5095–5115

Viterbo F, von Hardenberg J, Provenzale A, et al (2016) High-Resolution Simulations of the 2010 Pakistan Flood Event: Sensitivity to Parameterizations and Initialization Time. *J Hydrometeorol* 17:1147–1167. doi: 10.1175/JHM-D-15-0098.1

Annexure A: Seasonal precipitation trends at each station in d01, d02 and d03

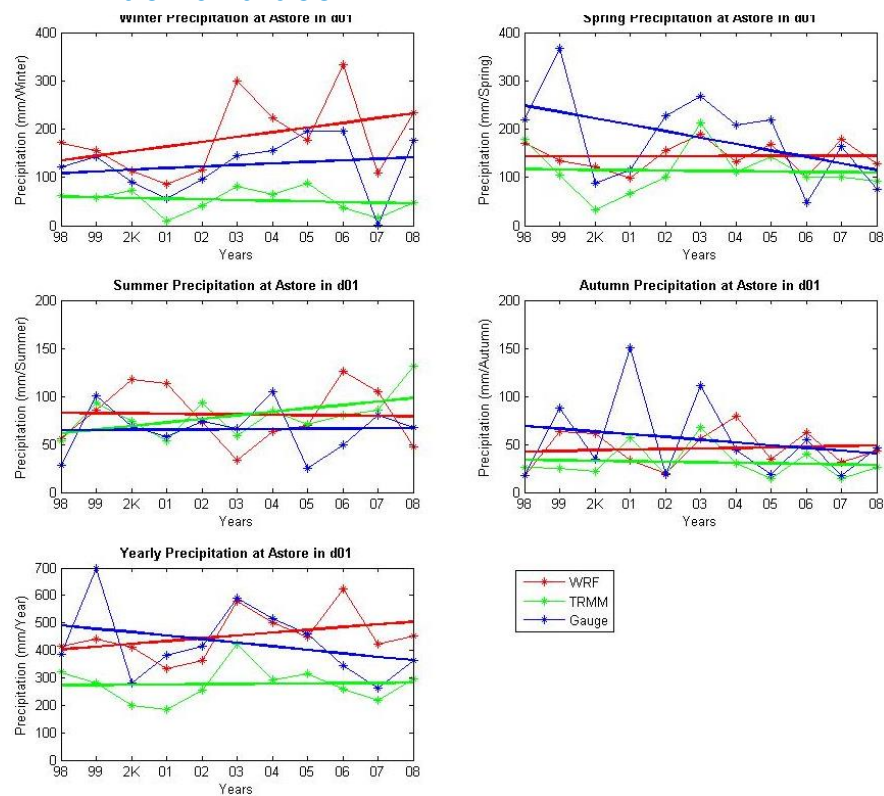


Fig. A1: Time series comparisons of precipitation between WRF, gauge and TRMM data at Astore station in domain-01 (d01).

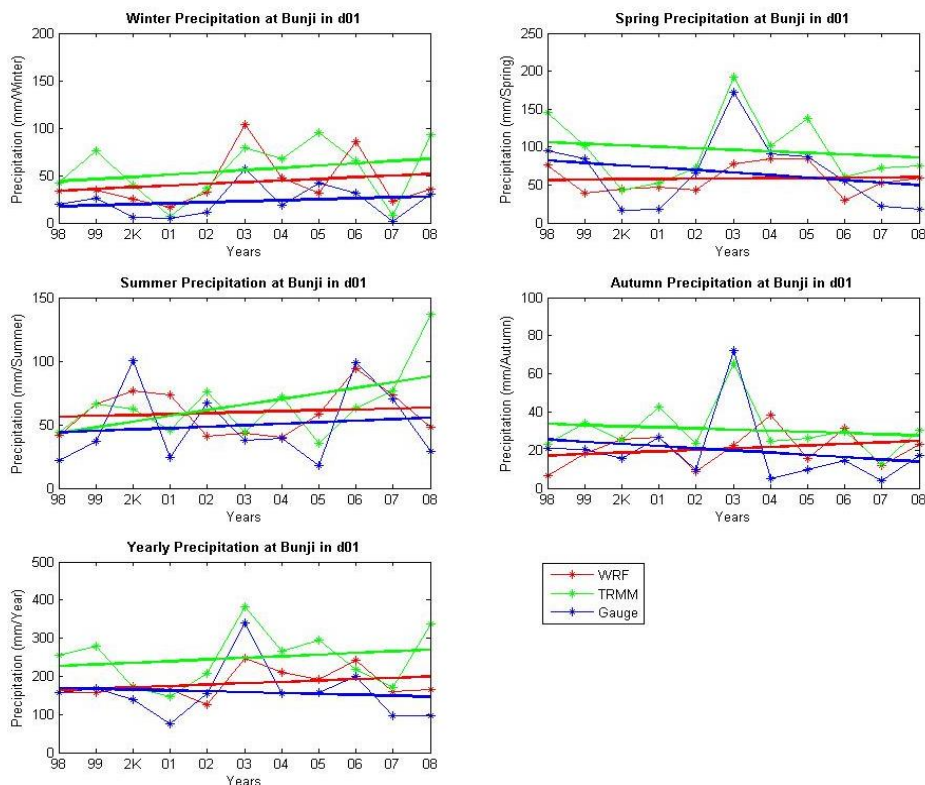


Fig. A2: Time series comparisons of precipitation between WRF, gauge and TRMM data at Bunji station in domain-01 (d01).

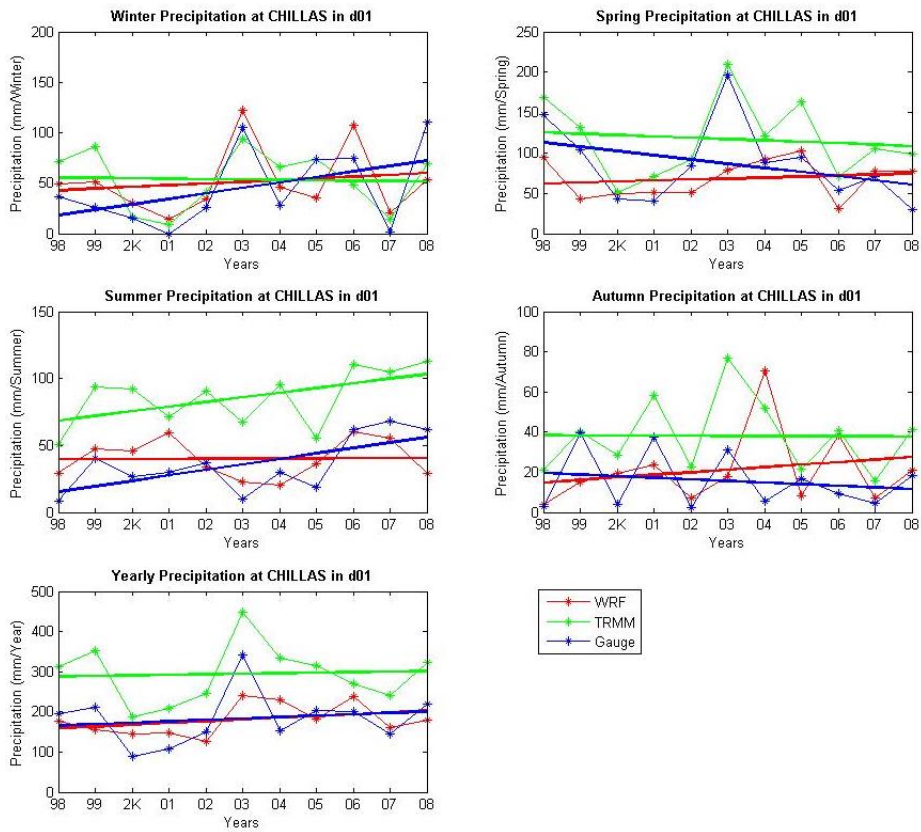


Fig. A3: Time series comparisons of precipitation between WRF, gauge and TRMM data at Chillas station in domain-01 (d01).

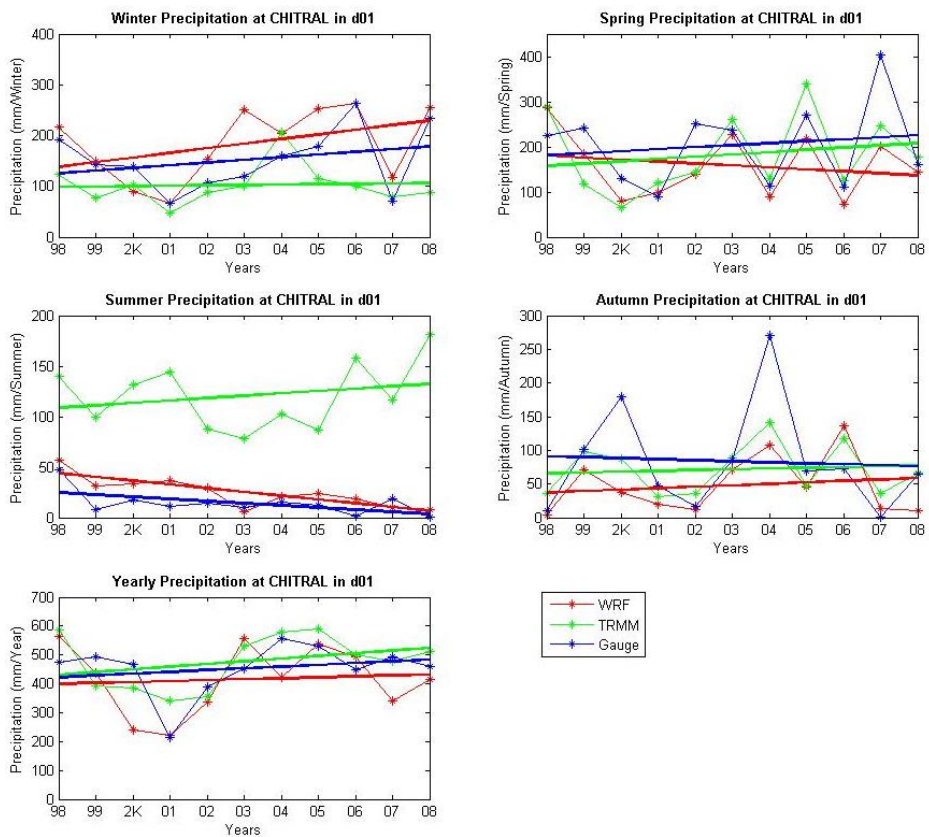


Fig. A4: Time series comparisons of precipitation between WRF, gauge and TRMM data at Chitral station in domain-01 (d01).

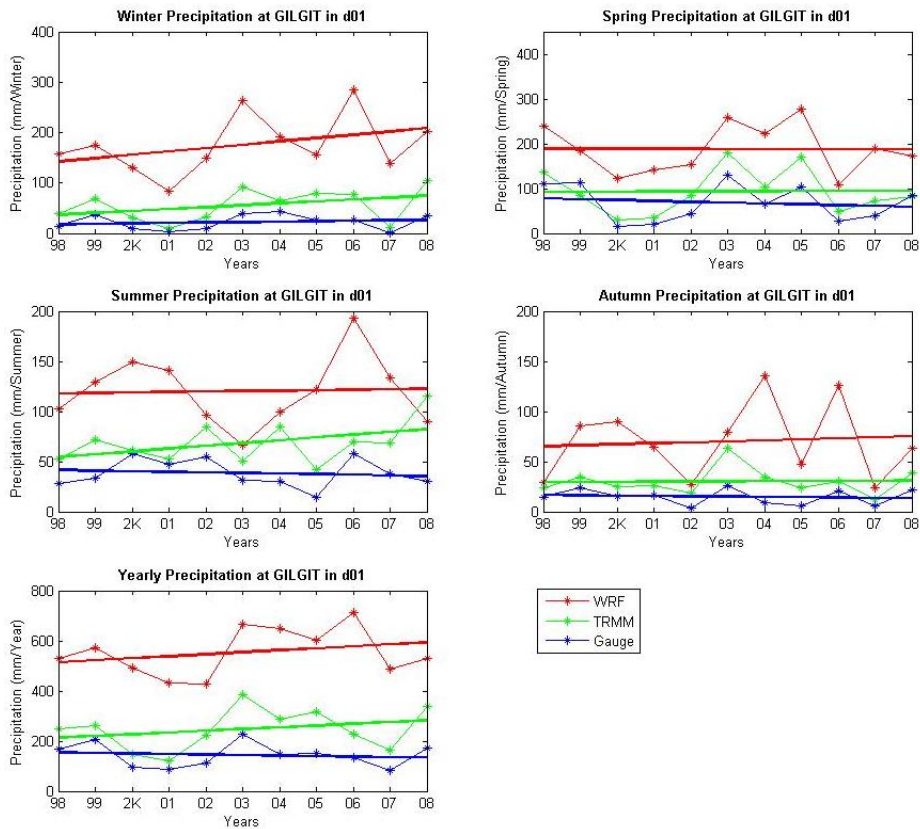


Fig. A5: Time series comparisons of precipitation between WRF, TRMM at Gilgit station in domain-01 (d01).

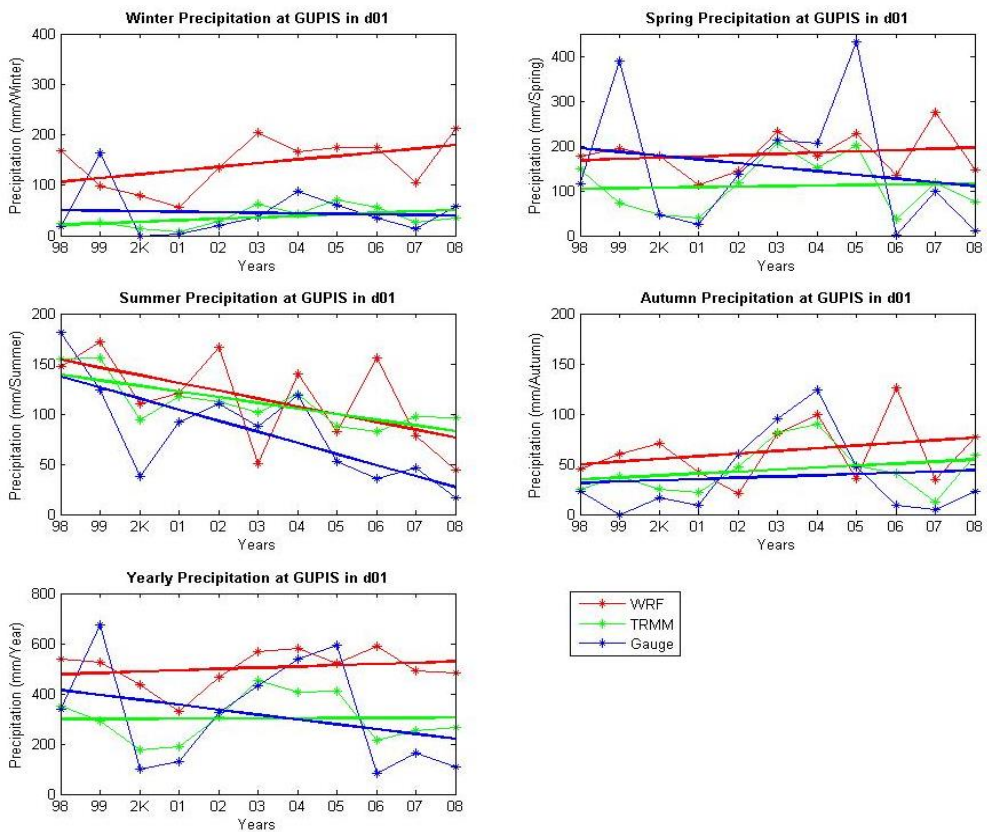


Fig. A6: Time series comparisons of precipitation between WRF, gauge and TRMM data at Gupis station in domain-01 (d01).

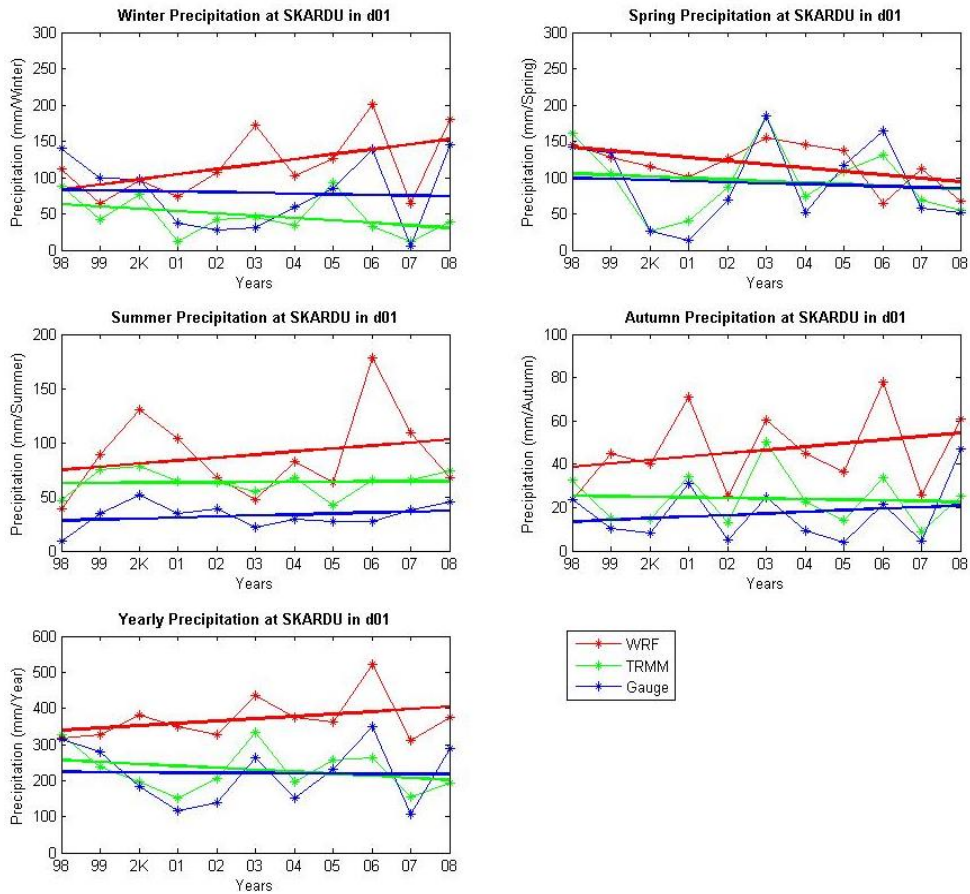


Fig. A7: Time series comparisons of precipitation between WRF, gauge and TRMM data at Skardu station in domain-01 (d01).

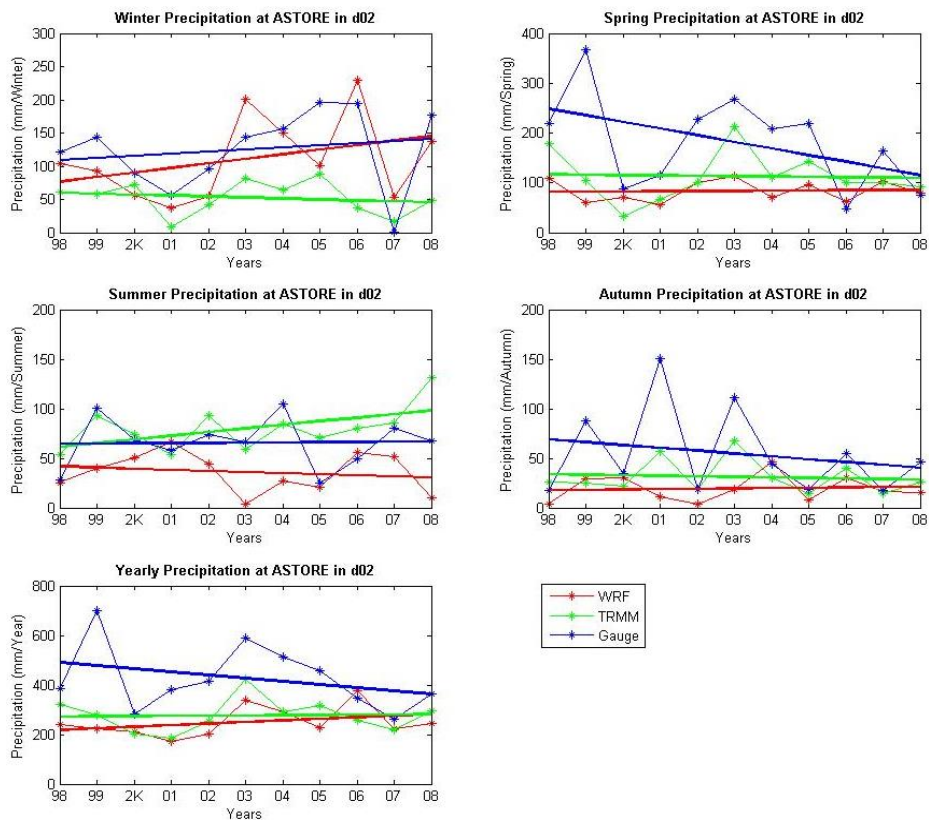


Fig. A8: Time series comparisons of precipitation between WRF, gauge and TRMM data at Astore station in domain-02 (d02).

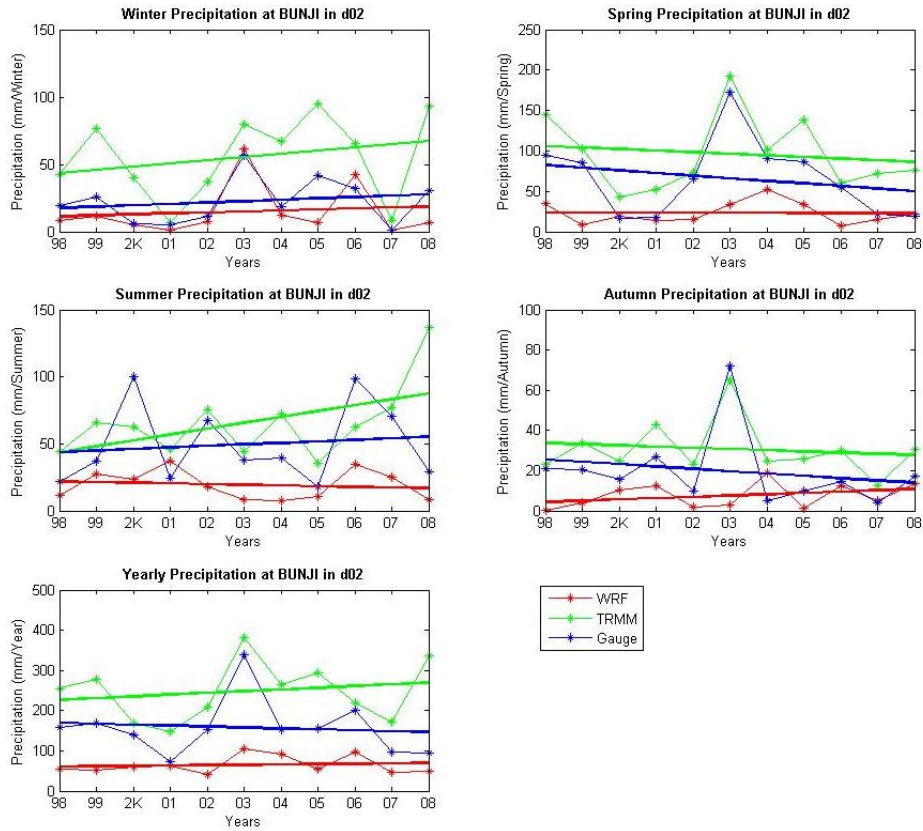


Fig. A9: Time series comparisons of precipitation between WRF, gauge and TRMM data at Bunji station in domain-02 (d02).

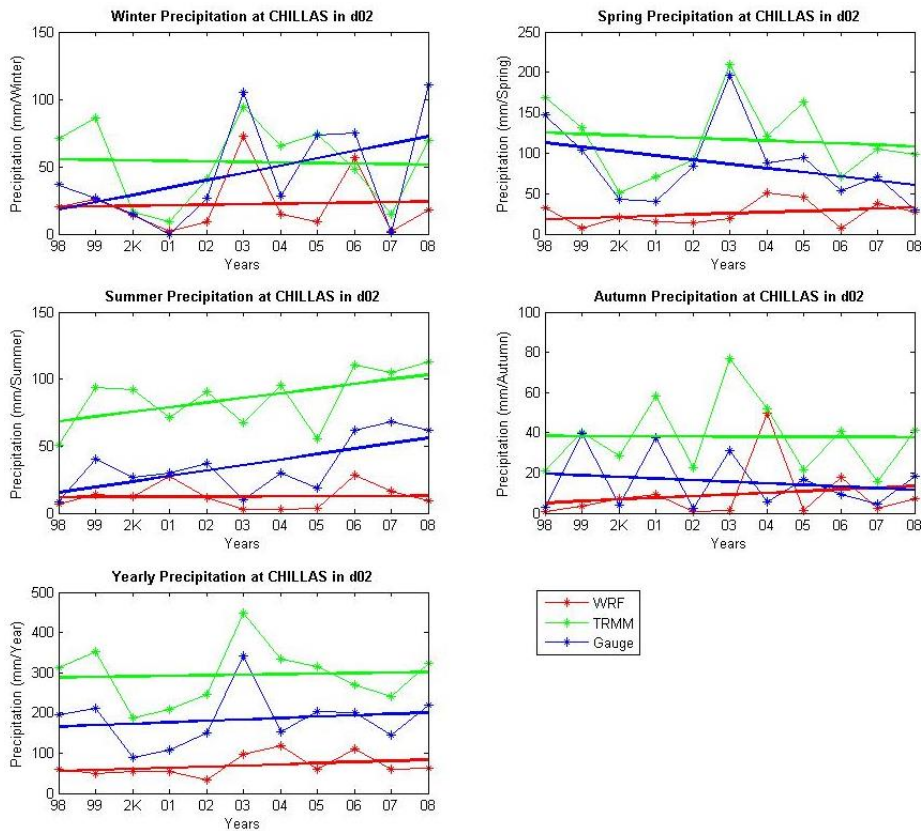


Fig. A10: Time series comparisons of precipitation between WRF, gauge and TRMM data at Chillas station in domain-02 (d02).

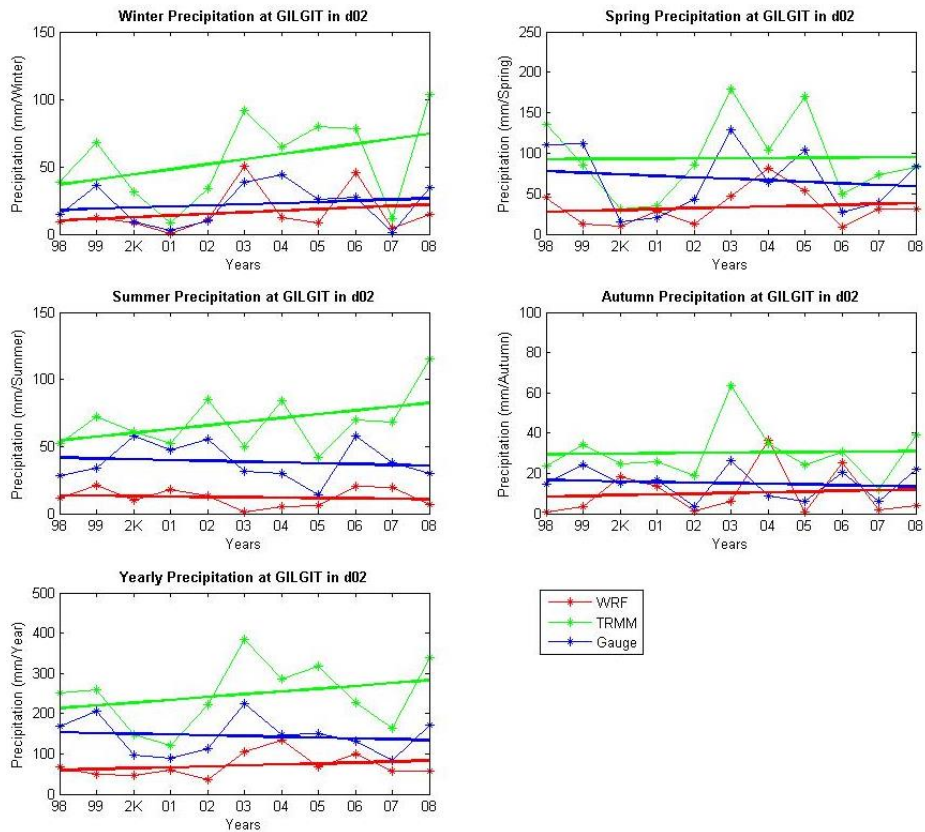


Fig. A11: Time series comparisons of precipitation between WRF, gauge and TRMM data at Gilgit station in domain-02 (d02).

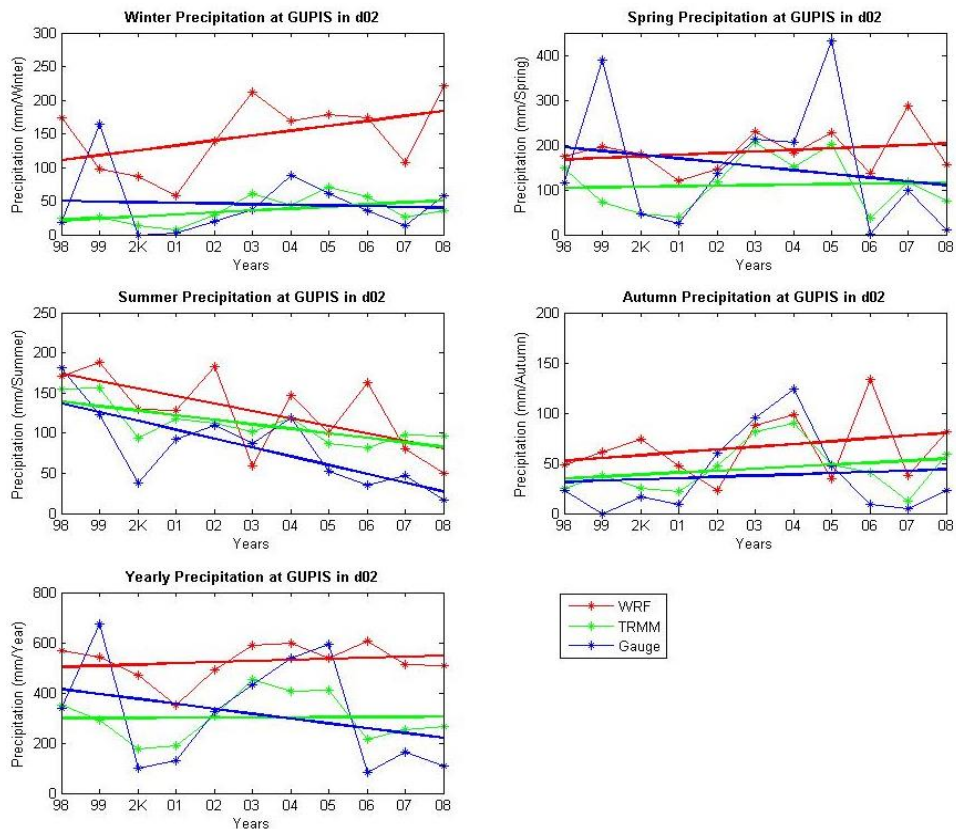


Fig. A12: Time series comparisons of precipitation between WRF, gauge and TRMM data at Gupis station in domain-02 (d02).

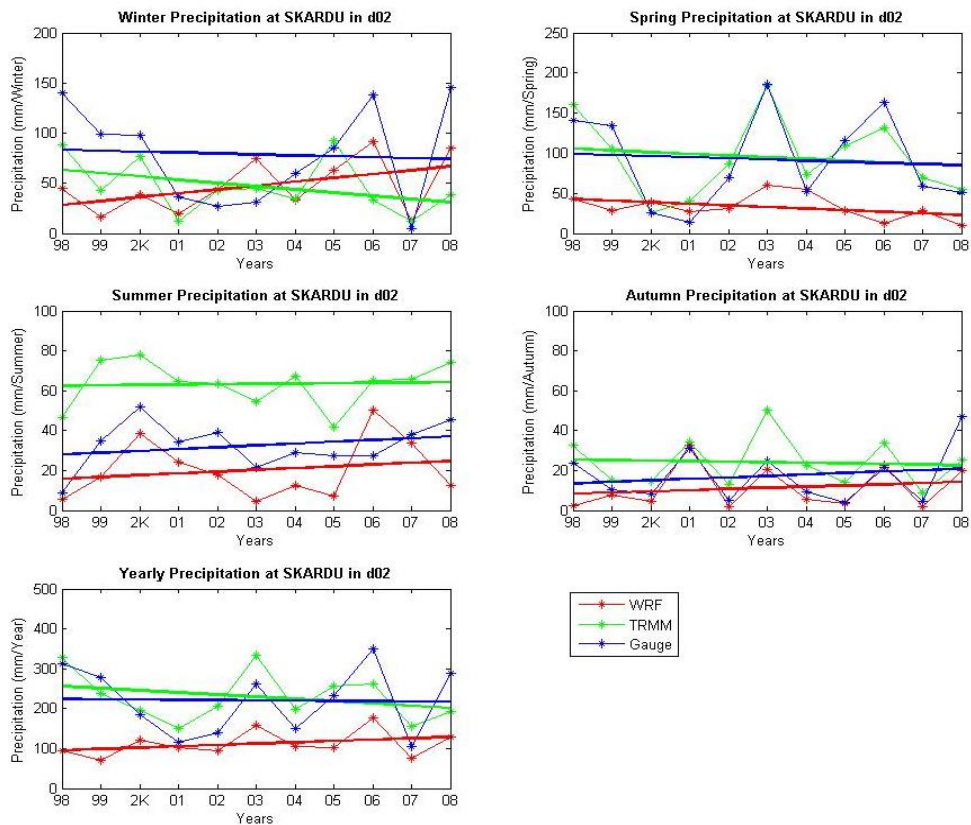


Fig. A13: Time series comparisons of precipitation between WRF, gauge and TRMM data at Skardu station in domain-02 (d02).

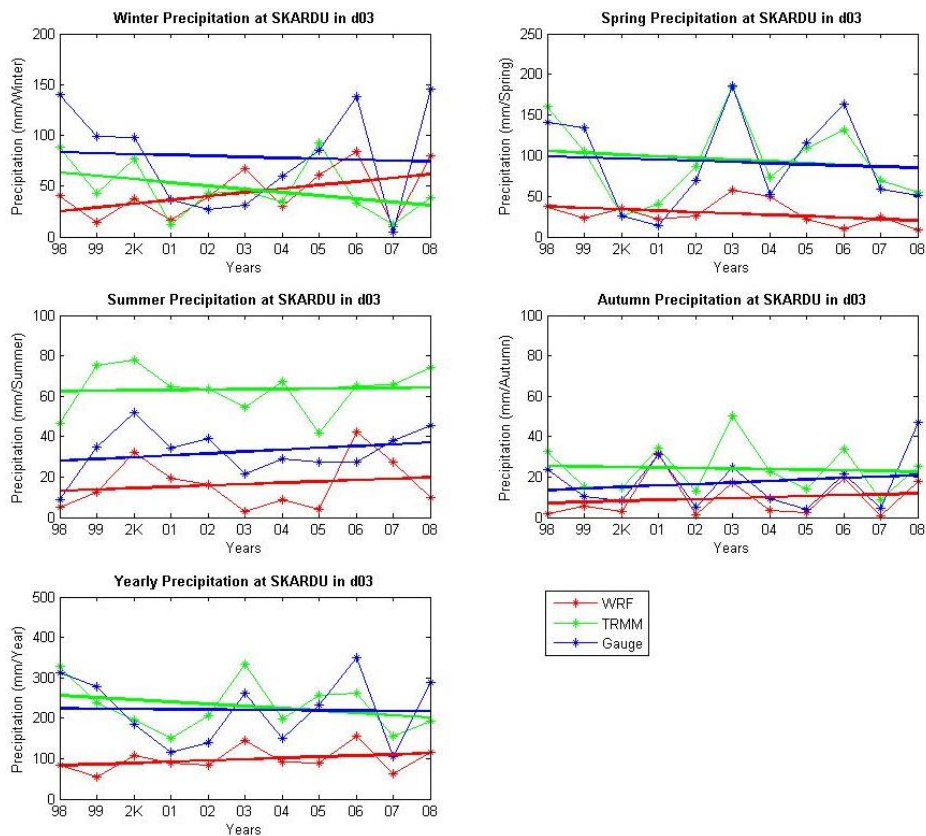


Fig. A14: Time series comparisons of precipitation between WRF, gauge and TRMM data at Skardu station in domain-03 (d03).

Annexure B: Year-wise precipitation trends at each station in d01, d02 and d03

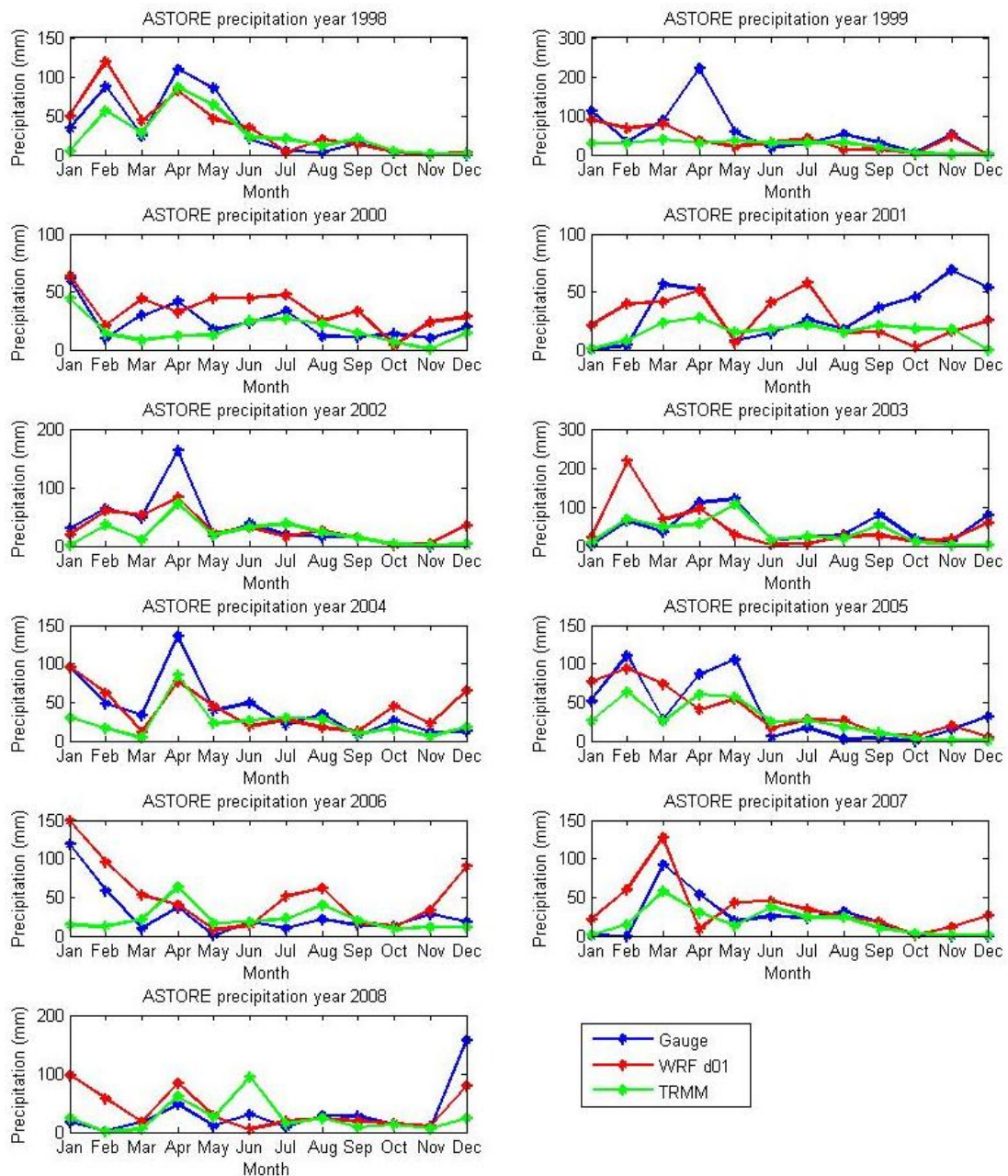


Fig. B1: Time series of precipitation comparisons between WRF, gauge and TRMM at Astore from 1998 to 2008 in d01.

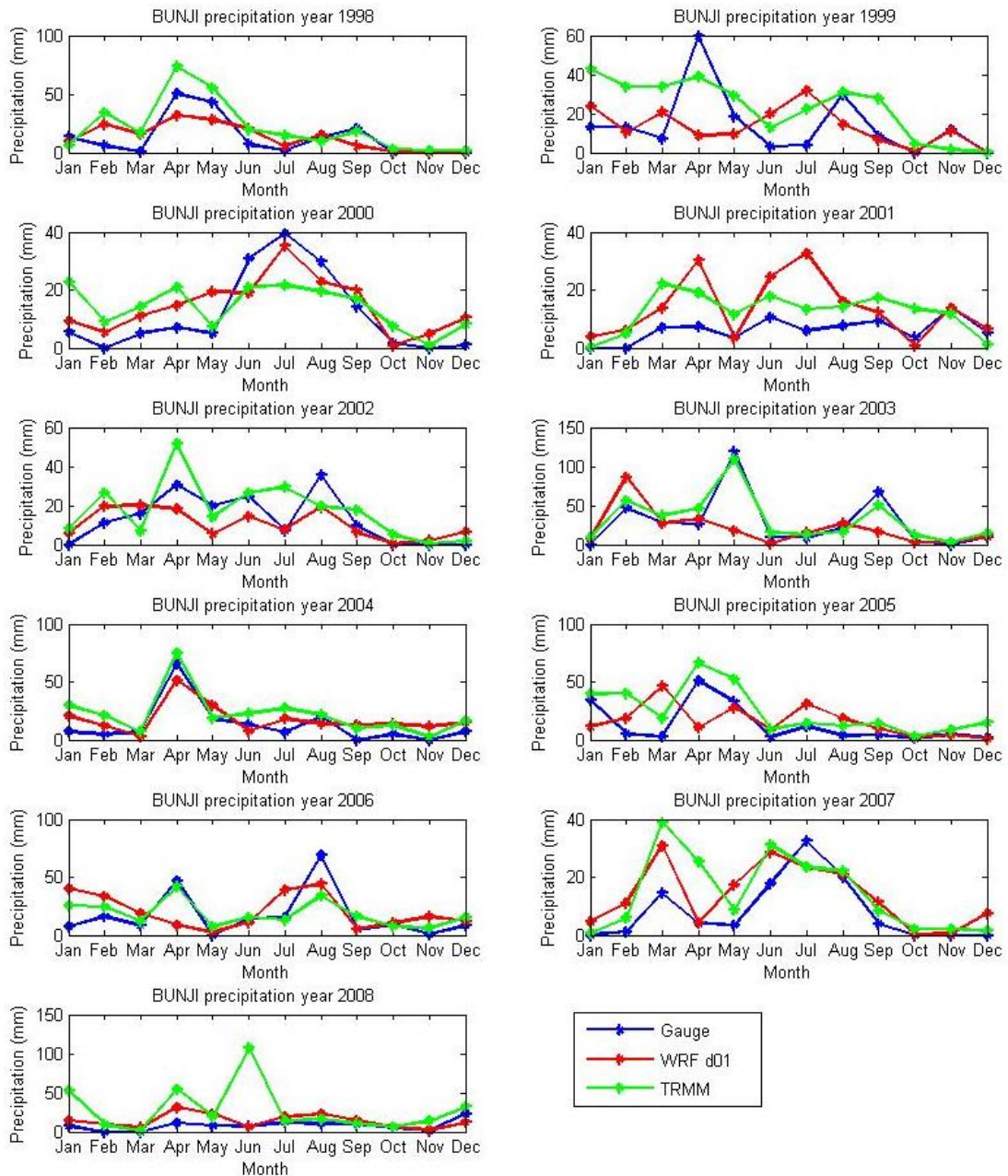


Fig. B2: Time series comparisons of precipitation between WRF, Gauge and TRMM at Bunji from 1998 to 2008 in d01.

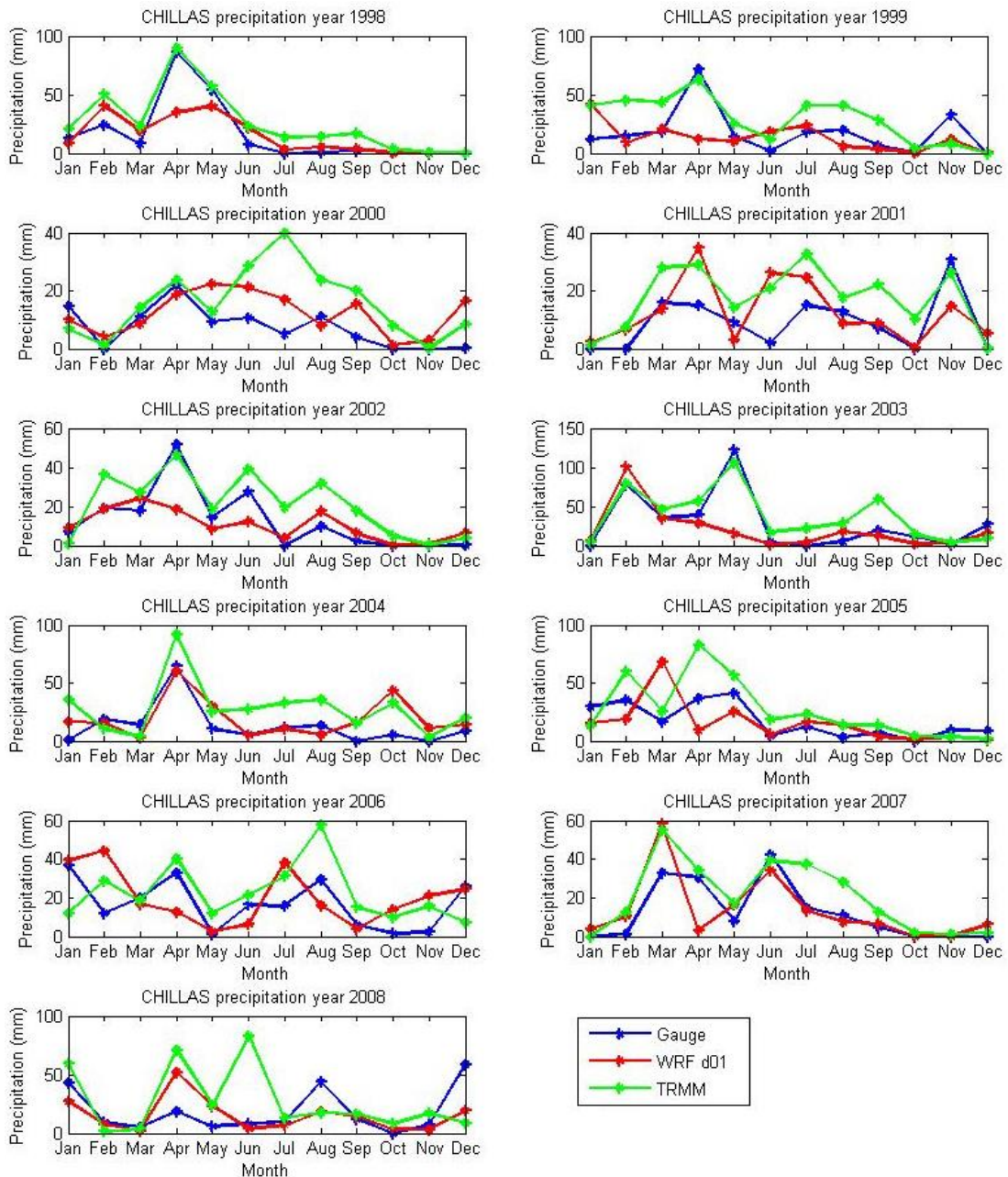


Fig. B3: Time series comparisons of precipitation between WRF, Gauge and TRMM at Chillas from 1998 to 2008 in d01.

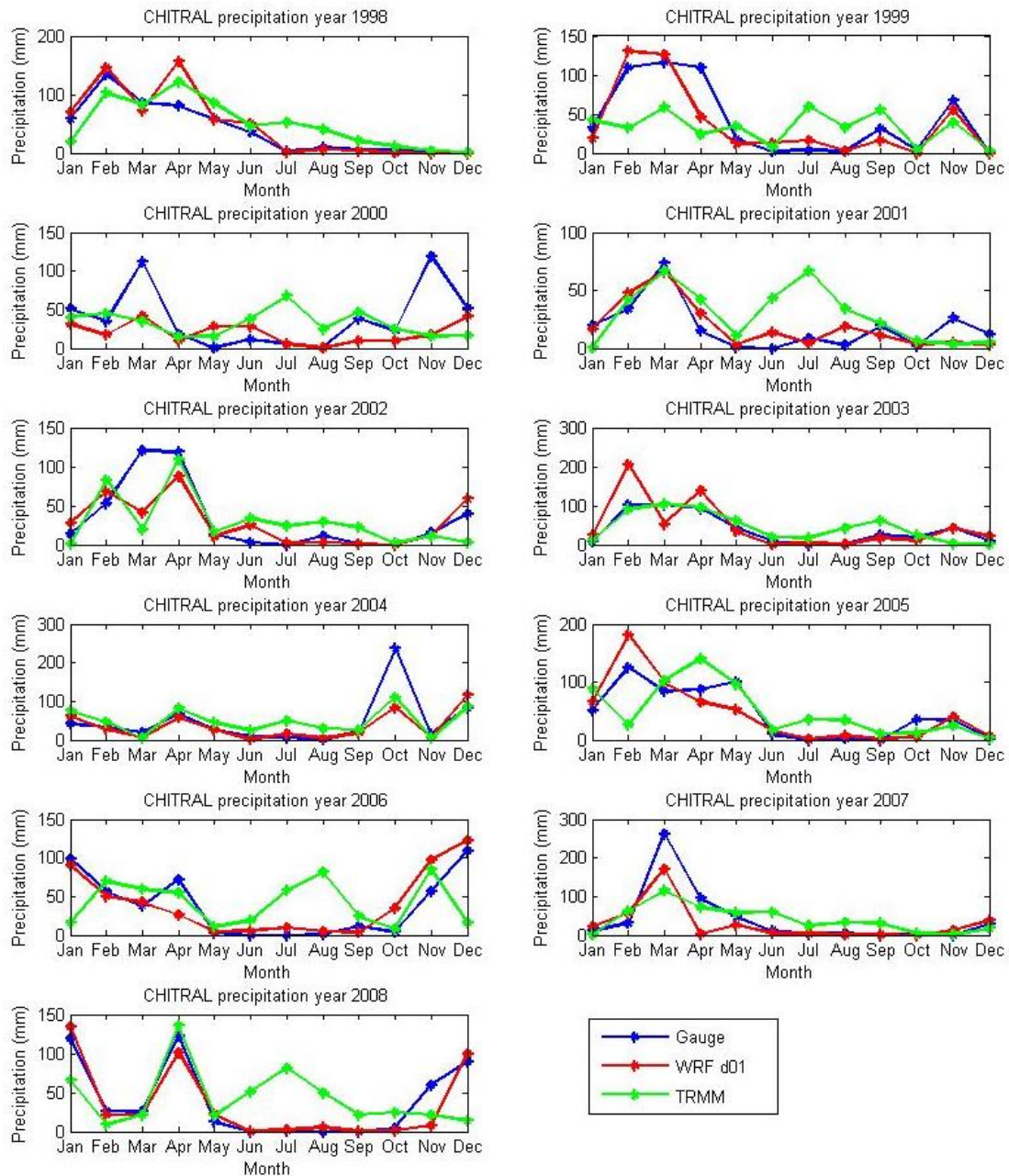


Fig. B4: Time series comparisons of precipitation between WRF, Gauge and TRMM at Chitral from 1998 to 2008 in d01.

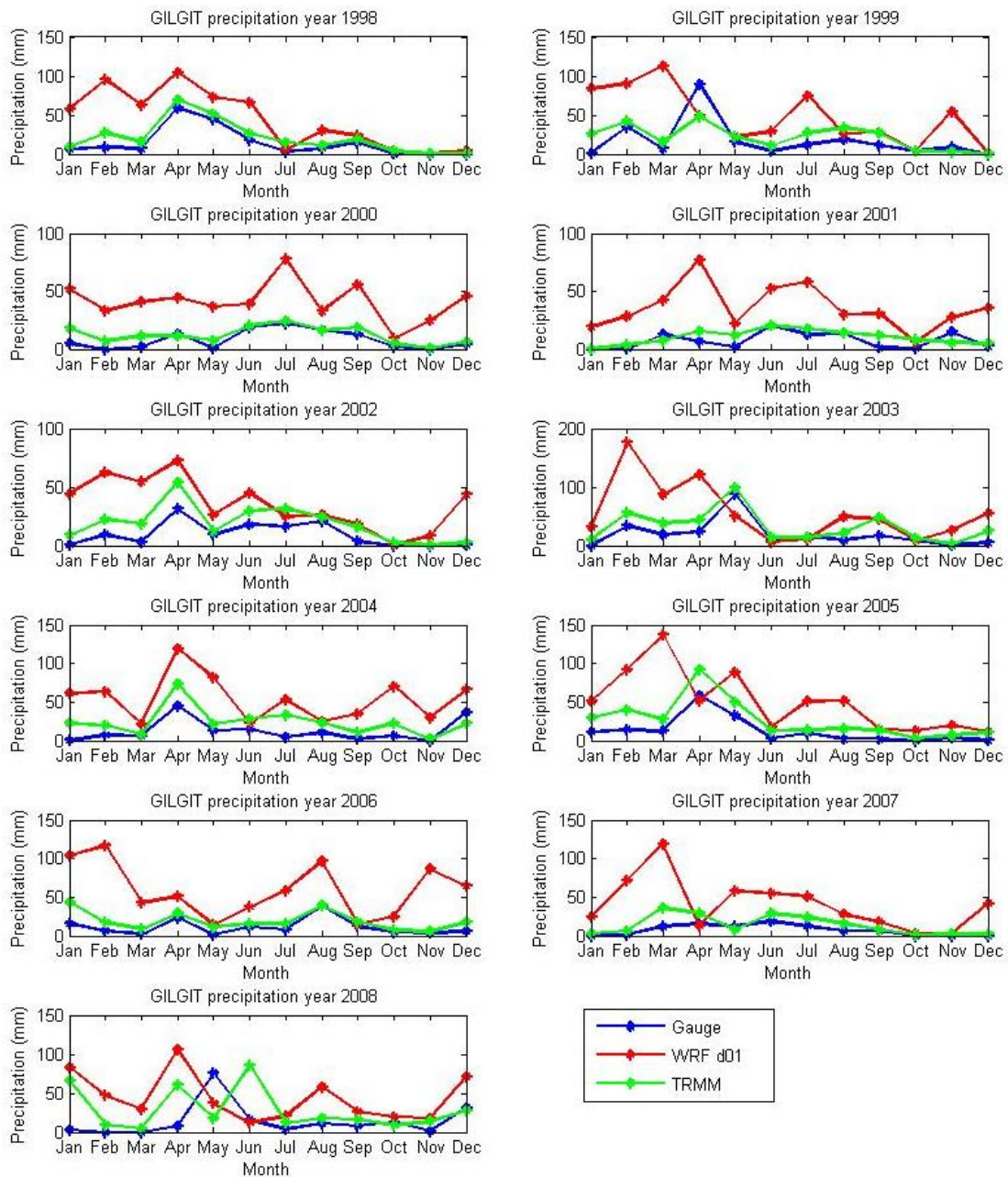


Fig. B5: Time series comparisons of precipitation between WRF, Gauge and TRMM at Gilgit from 1998 to 2008 in d01.

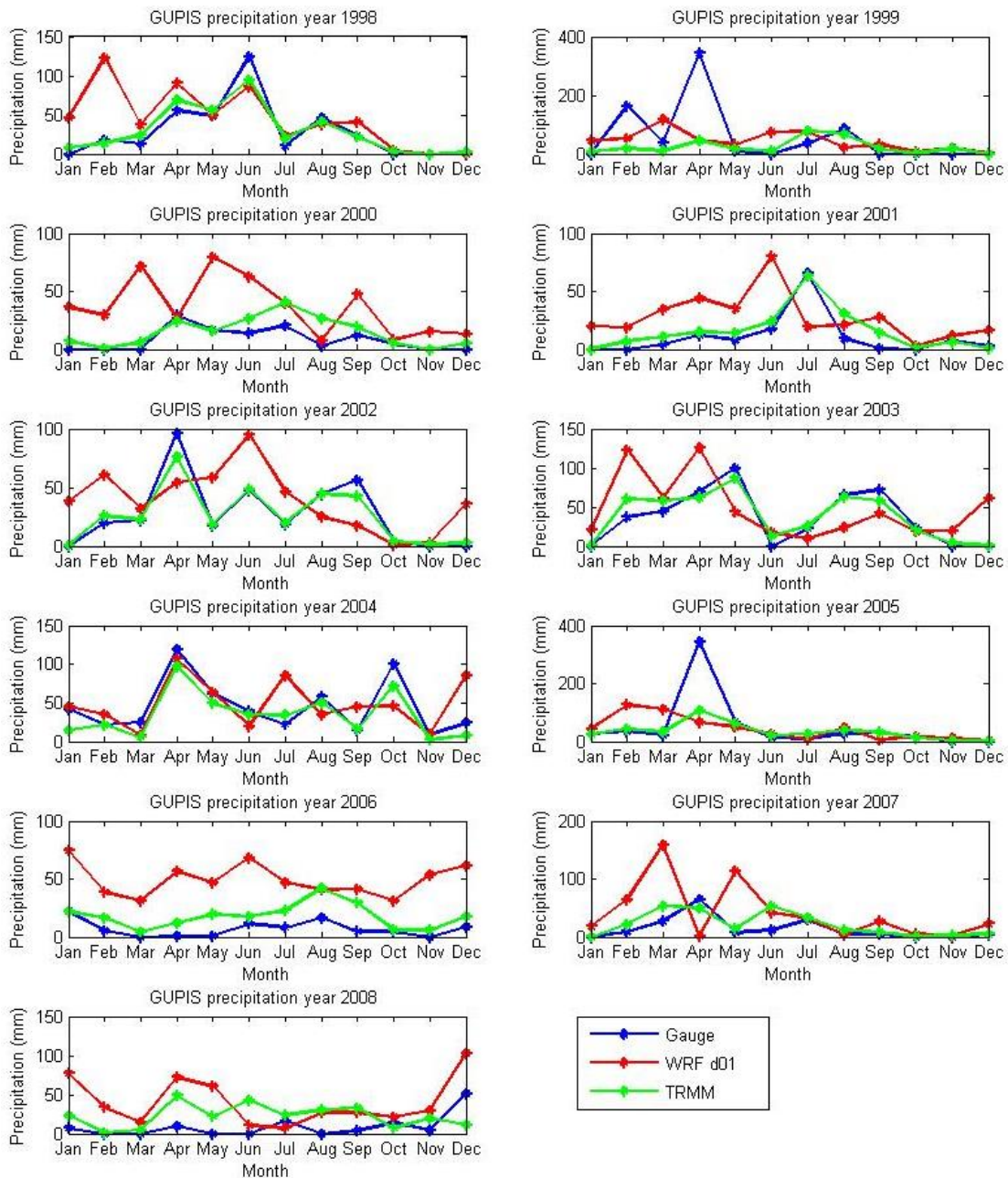


Fig. B6: Time series comparisons of precipitation between WRF, Gauge and TRMM at Gupis from 1998 to 2008 in d01.

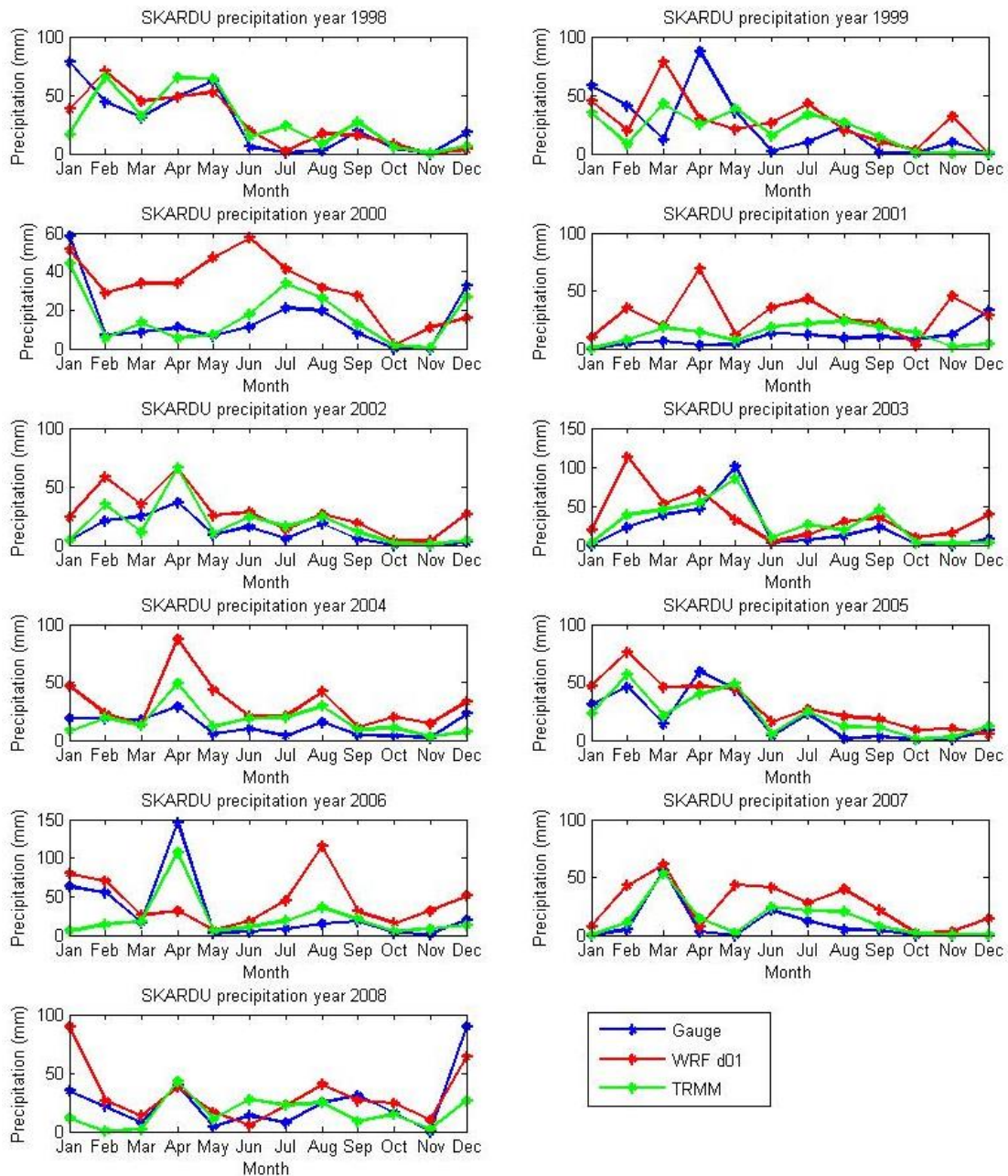


Fig. B7: Time series comparisons of precipitation between WRF, Gauge and TRMM at Skardu from 1998 to 2008 in d01.

Annexure C: Spatial yearly precipitation bias in d01, d02 and d03 from 1998-2008

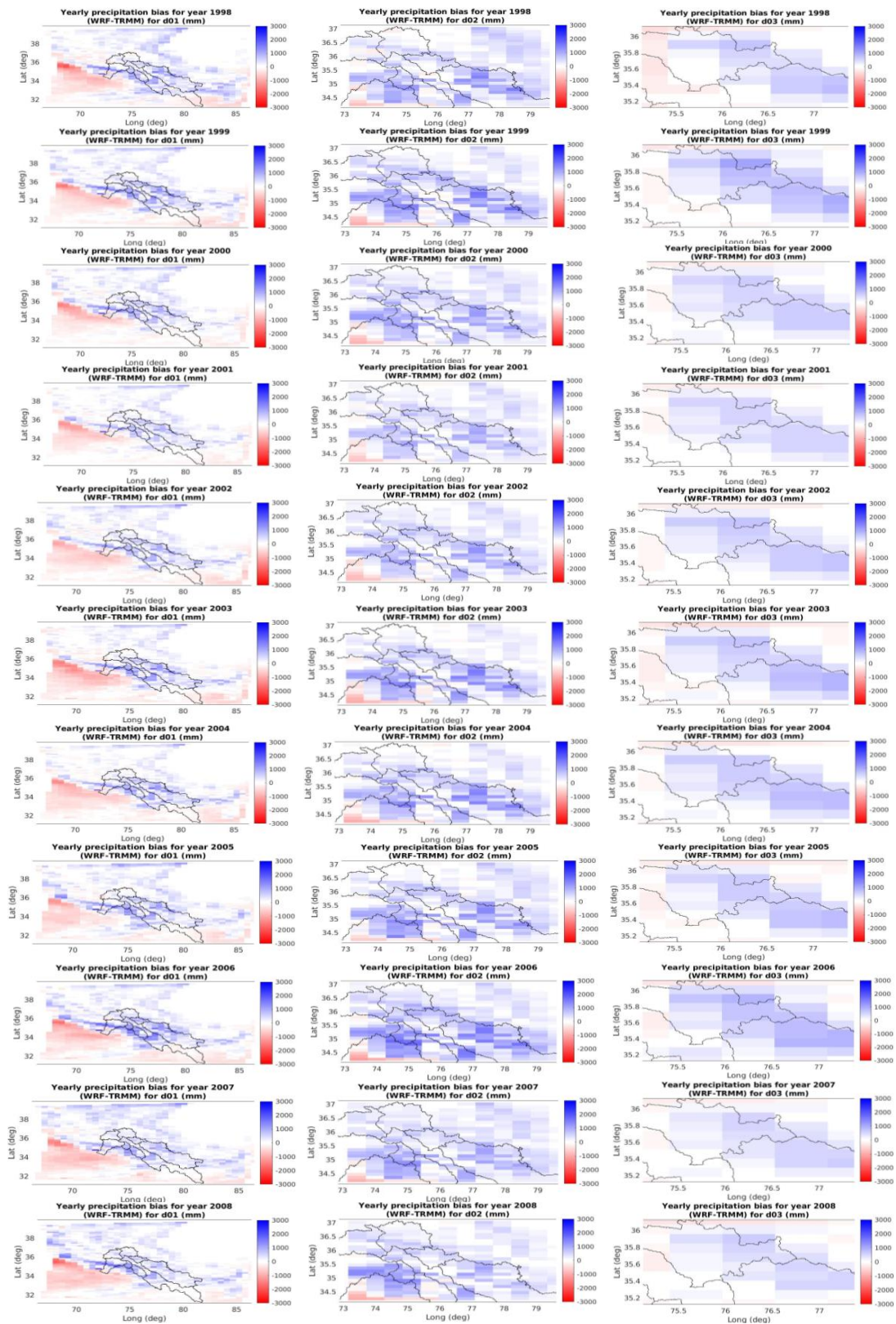


Fig. C1: Annual precipitation bias from 1998 through 2008 in all three domains. Left column shows annual precipitation bias for d01, middle column shows annual precipitation bias for d02, and right column shows annual precipitation bias for d03

Annexure D: Spatial yearly precipitation bias in d01, d02 and d03 for four simulations

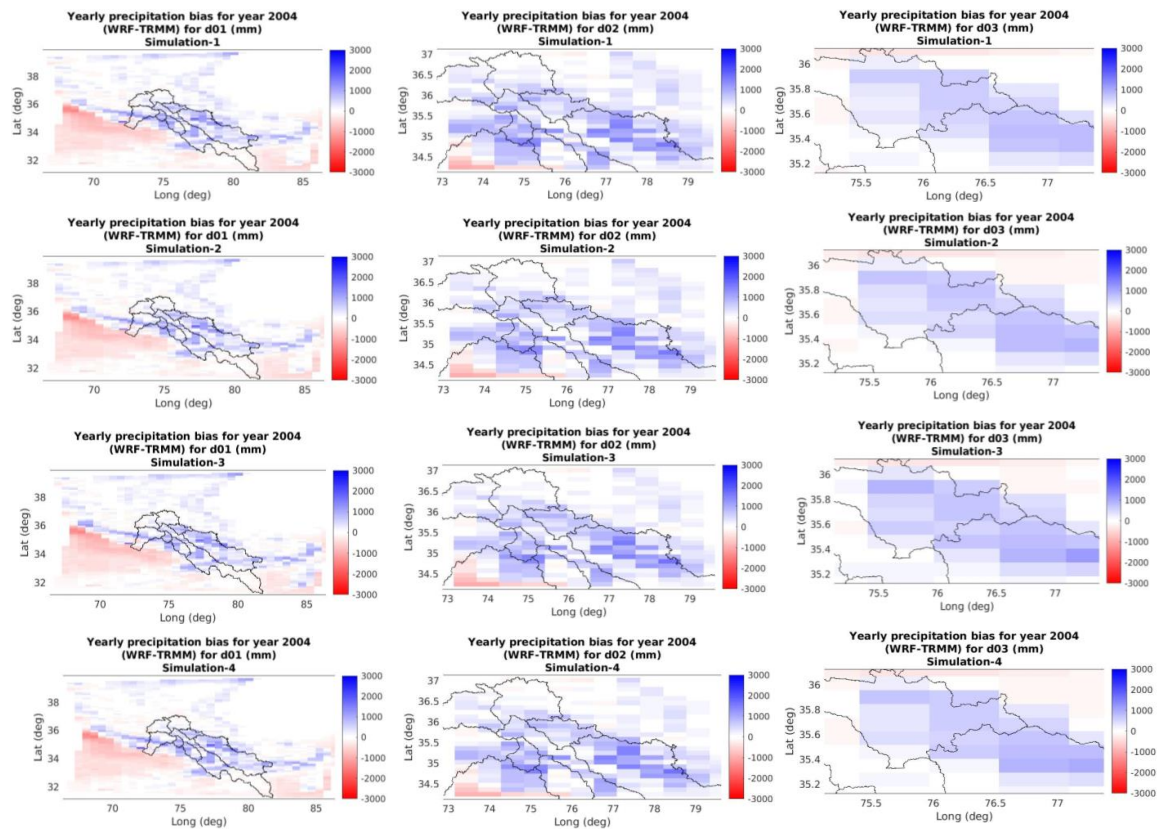


Fig. D1: Top row is simulation-1, second row is simulation-2, third row is simulation-3 and bottom row is simulation-4

About the Authors



Ghulam Hussain Dars is an Assistant Professor at the U.S.-Pakistan Center for Advanced Studies in Water (USPCAS-W), MUET, Jamshoro. He has 15 years experience in the planning, research, and teaching to his credit. Mr. Dars received a Fulbright Scholarship for MS degree in Civil and Environmental Engineering from Portland State University, Oregon, United States. He teaches the subjects Climate and Water, Hazards Planning and Risk Management, and Catchment Hydrology. He uses state-of-the-art tools (WRF-Hydro, SWAT, Matlab) to conduct research over Upper Indus Basin. His research interests include: Climate change impacts on water resources, statistical and dynamical downscaling, drought monitoring and forecasting, flood forecasting, uncertainty and risk analysis.

Dr. Court Strong is an Associate Professor with tenure in the Department of Atmospheric Sciences at the University of Utah. He is an expert in the simulation and analysis of climate dynamics with special interest in the cryosphere (the frozen portion of the climate system including mountain snowpack and sea ice). Dr. Strong is author on more than 50 peer-reviewed publications and has delivered more than 30 invited or keynote talks on climate. He is recipient of the American Geophysical Union James R. Holton Award for his research on climate dynamics and also a Top Researcher Award from the University of Utah. He teaches graduate and undergraduate courses in climate system physics and statistical climatology.



Dr. Adam Kochanski is a Research Assistant Professor at the University of Utah Atmospheric Sciences Department. He is an expert in high-performance computing and data analysis. He is an atmospheric modeler with extensive experience in running regional climate simulations as well as modeling of fire, smoke on high-performance computing platforms. Dr. Kochanski is an author on nearly 30 peer-reviewed publications and has delivered multiple invited or keynote talks. His research interests include impacts of regional climate on the hydrological cycle, as well as fire-atmosphere interactions including air quality impacts of wildland fires. He is a co-developer of the coupled fire-atmosphere model WRF-SFIRE, the integrated fire, and air quality system and WRF-SFIRE-CHEM, as well as the fire forecasting system WRFX. He is one of the modeling leads for the Fire and Smoke Model Evaluation Experiment (FASMEE) and a member of the Rocky Mountain Center for Fire-Weather Intelligence (RMC) steering committee.

Main thrust of Applied Research component of the Water Center is to stimulate an environment that promotes multi-disciplinary research within the broader context of water-development nexus to support evidence-based policy making in the water sector. This is pursued using the framework provided by the six targets of the Sustainable Development Goal on Water i.e. SDG-6.

Contact:

U.S.-Pakistan Centers for Advanced Studies in Water

Mehran University of Engineering and Technology, Jamshoro-76062, Sindh - Pakistan

 92 22 210 9145  water.mu.et.edu.pk  /USPCASW  /USPCASW